2. Materials and methods

2.1. Synthetic peptides

The Tax11-19 peptide, LLFGYPVYV, was purchased from Asahi Technoglass (Chiba, Japan) and used as an HLA-A2-restricted CTL antigen [11].

2.2. Cells

C1R.AAD cell line (HMYC1R transfected with HLA chimeric molecule containing α1 and α2 domains from human HLA-A2.1 and α3 from mouse H-2D^d) was described previously [22]. Cell lines were maintained in culture medium (CTM; 1:1 mixture of RPMI 1640 and Eagle-Hank's amino acid (EHAA)) containing 10% fetal bovine serum (FBS), 1 mM sodium pyruvate, 0.1 mM nonessential amino acids, 10 mM HEPES, 4 mM glutamine, 100 U/ml penicillin, and 100 μg/ml streptomycin.

HTLV-1-infected human ATL cell lines, KK-1 and KOB, were derived from the peripheral blood and ascites of ATL patients, respectively [23,24]. Human IL-2 dependent T cell line (HCT-4) was derived from the cerebrospinal fluid of a HAM/TSP patient [25]. KK-1, KOB, and HCT-4 were used as a target. Cells were maintained in CTM with 100 units/ml of recombinant human IL-2 (Imunace®35, Shionogi, Osaka, Japan).

2.3. Mice

Transgenic HHD-2 mice (gift from Dr. François Lemonnier, Institute Pasteur, Paris, France) were bred in our colony at the Institute of the Experimental Animals at St. Marianna University. HHD-2 mice are characterized by knock-out of the murine β_2-microglobulin gene, as well as murine H-2D^b, transgenic expression of human HLA-A2.1 with a covalently-linked human β_2-microglobulin and a murine D^b-derived α3 domain to allow interaction with mouse CD8 [26]. All animal studies were approved by the Institute of Experimental animals at St. Marianna University.

2.4. Binding assay

Peptide binding to HLA-A2 molecules was measured using T2 mutant cell lines as described previously [27,28]. T2 cells (3×10^5/well) were incubated overnight in 96-well plates with culture medium (a 1:1 mixture of RPMI 1640 and Eagle-Hank's amino acid (EHAA) containing 2% FBS, 100 U/ml penicillin, 100 mg/ml streptomycin) with 10 μg/ml human β_2-microglobulin (Sigma–Aldrich, St. Louis, MO) and different peptide concentration. On the following day, cells were washed at 190 × *g* for 5 min twice with cold PBS containing 2% FBS and incubated for 30 min at 4 °C with anti-HLA-A2.1 BB7.2 mAb (1/100 dilution of hybridoma supernatant) and 5 μg/ml FITC-labeled goat anti-mouse Ig (BD PharMingen, San Diego, CA). Cells were washed twice after each incubation; subsequently, HLA-A2.1 expression was measured by flow cytometry (FACScan; BD Biosciences, Mountain View, CA). HLA-A2.1 expression was quantified as fluorescence index (FI) according to the formula: FI = ((geometric mean fluorescence with peptide − geometric mean fluorescence without peptide)/geometric mean fluorescence without peptide). $FI_{0.5}$ is the concentration required to give an FI of 0.5, meaning a 50% increase in HLA-A2 on the cell surface. Background fluorescence without BB7.2 was subtracted for each individual value. To compare the different peptides, $FI_{0.5}$ was calculated from the titration curve for each peptide. Each sample was tested in triplicate. Values were expressed as mean in triplicate.

2.5. CTL generation in HHD-2 transgenic mice

The method for generating antigenic peptide-specific CTL lines form HHD mice was described previously [28,29]. Mice aged more than 8 weeks were immunized subcutaneously in the base of the tail with 100 μl of an emulsion containing 1:1 incomplete Freund's adjuvant (IFA), antigenic CTL peptide and cytokines (50 nmol Tax (11-19) peptide, 25 nmol HBV core 128–140 helper epitope, 3 μg of rmIL-12 and 3 μg of rmGM-CSF). Mice were boosted 2 weeks later, with the spleens removed 10–14 days after the boost. Immune spleen cells (2.5×10^6/well) were stimulated in 24-well plates with autologous spleen cells (5×10^6/well) pulsed for 30 min with 10 μM Tax11-19 peptide for the development of low-avidity CTL lines (LCTL) or with 10 nM for high-avidity CTL lines (HCTL) in CTM supplemented with 10% T-stim® (Collaborative Biochemical Products, Bedford, MA). Following a minimum of four in vitro stimulations with the peptide-pulsed syngeneic spleen cells, two CTL lines were maintained by weekly restimulation with 1×10^6 cells/well with 4×10^6 peptide-pulsed mitomycin C-treated syngeneic spleen cells as feeders.

2.6. Cytotoxic assay

CTL activity was measured with ^{51}Cr-labeled target cells. Target cells (1×10^6) were pulsed in 100 μl of 150 μCi ^{51}Cr for 1 h and were washed three times, with 5000 cells/well then added to 96-well round-bottom plates containing different peptide concentrations. Effector cells were introduced followed by additional incubation. Supernatants were then harvested and analyzed. The percentage of specific ^{51}Cr release was calculated as 100 × (experimental release − spontaneous release)/(maximum release − spontaneous release). Spontaneous release was determined from target cells that had been incubated in the absence of effector cells, while maximum release was determined in the presence of 2% TRITON® X-100 Detergent (CALBIOCHEM, La Jolla, CA). Each sample was tested in triplicate. Values were expressed as means ± SEM of triplicates.

2.7. IFN-γ ELISA assay

IFN-γ in the culture supernatant harvested at 24 h was determined using an ELISA kit (R&D, Minneapolis, MN) according to the manufacture's instructions. All samples were analyzed in triplicate. Values were expressed as means ± SEM of triplicates.

2.8. TCR Vβ screenings of CTLs

We assessed a Vβ usage pattern between HCTL and LCTL using Vβ TCR screening kit by a flow cytometry analysis (BD Bioscience Phamingen, San Diego, CA).

2.9. Flow cytometry

We used a PE-Tax11-19/HLA-A*0201 tetramer-LLFGYPVYV (Medical & Biological Laboratories, Nagoya, Japan) and PE-hamster anti-mouse CD3ε Ab (145-2C11, BD Bioscience Phamingen, San Diego, CA). Cells were centrifuged and washed twice with PBS containing 0.5% BSA, and then resuspended in 1% BSA/PBS. Cells were incubated 40 min at 4 °C with the antibody and then washed three times. The tetramer and anti CD3ε Ab were titrated for staining simultaneously.

In order to compare the affinity of T cell receptor between HCTLs and LCTLs, indexes were calculated using the following two equations: ratio of geometric mean (RGM) = (geometric mean using tetramer or anti-CD3ε Ab)/(geometric mean using control Ab). Each sample was tested in triplicate.

2.10. Western blotting

KK-1, KOB, and HCT-4 were lysed using standard lysis buffer (20 mM Tris–HCl, 250 mM NaCl, 1% NP-40, 1 mM dithiothreitol, 10 mM NaF, 2 mM Na_3VO_4, 10 mM $Na_4P_2O_7$, and protease inhibitor cocktail (Roche, Mannheim, Germany)). Lysates were stored at −80 °C until use. Protein concentration was determined using the Bradford method (Bio-Rad protein assay reagent; Bio-Rad laboratories, Hercules, CA). Equal amounts (30 μg) of protein were separated by SDS–PAGE on 10% polyacrylamide gels and transferred to PVDF membranes. Following the transfer, membranes were blocked with Difco Skim milk (BD Bioscience, San Diego, CA) overnight at 4 °C. The working concentrations of the first Abs were 1 μg/ml for anti-Tax Ab (Lt-4) [30] and anti murine β-actin Ab (SIGMA, St. Louis, MO), and 1:10,000 for HRP-conjugated anti-mouse IgG Ab (SIGMA, St. Louis, MO). The membrane was washed, and was reacted with the appropriate second antibody. Finally, signals were visualized using the extended cavity laser (ECL) system (GE Healthcare Bio-sciences KK, Tokyo, Japan).

2.11. Real-time reverse transcriptase-PCR (RT-PCR)

Total RNA was isolated from cells using TRIzol® Reagent (Invitrogen, Carisbad, CA). First-stand cDNA was synthesized with random hexamers and reverse transcriptase (ReverTraAce; Toyobo, Japan) using 1 μg of total RNA in a reaction volume of 20 μl. Real-time PCR reactions were carried out using TaqMan® Universal Master Mix (Applied Biosystems, Carisbad, CA). ABI Prism 7500 SDS was programmed to an initial step of 2 min at 50 °C and 10 min at 95 °C, followed by 45 cycles of 15 s at 95 °C and 1 min at 60 °C. The primers and probe for detecting the HTLV-1 Tax or GAPDH mRNA were used as described previously [31]. Relative quantification of mRNA was performed using the comparative threshold cycle method with GAPDH as an endogenous control. For each sample, target gene expression was normalized against the expression of GAPDH. To determine relative expression levels, the following formula was used: target gene expression = $2^{-(Ct[target]-Ct[GAPDH])}$. Each sample was tested in triplicate. Values were expressed as means ± SEM of triplicates.

3. Results

3.1. Binding affinity of Tax11-19 for HLA-A2 molecule

Before attempting to develop Tax-specific CTL lines from HLA-A2 transgenic HHD mice, we evaluated the binding affinity of Tax11-19 peptide by T2 binding assay, which measures the cell surface stabilization of HLA-A2 molecules. Tax11-19 peptide displayed a binding capacity for the HLA-A2 molecule that was nearly equal to that of the positive control, the highly antigenic influenza virus matrix peptide (FMP58-66) [32] ($FI_{0.5}$ = 0.329 for Tax11-19, 0.284 μM for FMP58-66) (Fig. 1). These data suggest that Tax11-19 would be a very strong antigenic peptide restricted to the HLA-A2 molecule.

3.2. Recognition of Tax11-19 peptide by CTL lines of different avidity

Based on the observation that Tax11-19 showed strong antigenicity inducing specific CTLs, we next attempted to develop low-avidity CTLs (LCTL) and high-avidity CTLs (HCTL) from HLA-A2 transgenic mice. HCTL were generated by weekly stimulation using low concentrations (10 nM) of the Tax peptide pulsed onto APCs, while LCTLs were also generated using 10 μM of the Tax peptide pulsed onto APCs. Using these different CTL lines, we examined Tax-specific CTLs-mediated cytotoxicity with Tax peptide titrated over a range of concentrations. The titration curve showed a

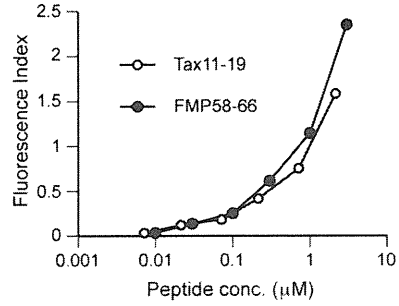

Fig. 1. Comparison of HLA-A2 binding curves between Tax11-19 and FMP58-66 peptide in T2-binding assay. The binding affinity of Tax11-19 for HLA-A2 molecule is almost as strong as that of FMP58-66 in influenza A virus.

0.5–1 $\log_{10}$ difference in functional avidity measured as the peptide concentration necessary to produce 50% lysis (Fig. 2A). Similarly, we examined their properties in antigen-specific IFN-γ production from these CTL lines (Fig. 2B). With a 24 h assay, HCTLs showed more IFN-γ production than LCTLs even at lower concentration of Tax antigen. These data suggest that the two different CTL lines specific for Tax have different functional avidity.

3.3. Different Vβ usage and binding ability to Tax-tetramer between high- and low-avidity CTLs

In order to confirm whether these CTLs with different avidity possessed different TCR structures, we assessed the difference in Vβ usage pattern between HCTLs and LCTLs using flow cytometric analysis (FCM). On FCM, antibodies available for screening were those for Vβ 2, 3, 4, 5, 6, 7, 8.1, 8.2, 8.3, 9, 10, 11, 12, 13, 14, and 17. On FCM, no Vβ were detected in LCTLs, while only Vβ5 was detected in HCTLs (Fig. 3A). The data suggested that the major TCR repertoire of HCTL is Vβ5, indicating that these two Tax-specific CTL lines have different TCR structures.

We next compared the binding affinity of TCR between HCTL and LCTL using Tax11-19/HLA-A2 tetramer-LLFGYPVYV and anti-CD3 Ab (Fig. 3B). On FCM with both Tax11-19-tetramer and anti-CD3 Ab titration, HCTLs showed a stronger fluorescence than LCTLs (Fig. 3B). On Tax11-19-tetramer assay, the ratio of fluorescence index (HCTL/LCTL) was ~5-fold at any titrated concentration, and it took 1.5 logs more tetramer to achieve the same level of staining. In the titration of anti-CD3 Ab, the ratio was ~3-fold and also it required about 3-fold more antibody to reach the same level of staining. These findings suggested that HCTLs not only have higher TCR affinity but also express greater numbers of TCR molecules on their surface when compared with LCTLs.

3.4. Recognition of human ATL targets by Tax-specific CTLs from HHD mice

We further examined whether these murine CTL lines with different functional avidity could induce cytotoxic activity against human ATL targets. We used the HTLV-1-infected human ATL cell lines, KK-1 (HLA-A2) and KOB (HLA-A30) as target cells derived from peripheral blood and ascitis of ATL patients, respectively [23,24]. These murine CTL lines did not show strong cytotoxicity against human ATL lines as against murine targets with a 4 h assay, as it was previously reported that species specificity between murine CD8 and the α3 domain of human HLA-A2 may reduce the recognition ability by CTLs [33]. However, on a 12 h assay, cytotoxicity against human ATL was observed in an HLA-A2 restricted manner (Fig. 4A). HCTLs were especially more efficient at killing at low E/T ratios. Furthermore, on kinetics assay, HCTLs showed more efficient cytotoxicity against the human ATL target (KK-1) than LCTLs (Fig. 4B).

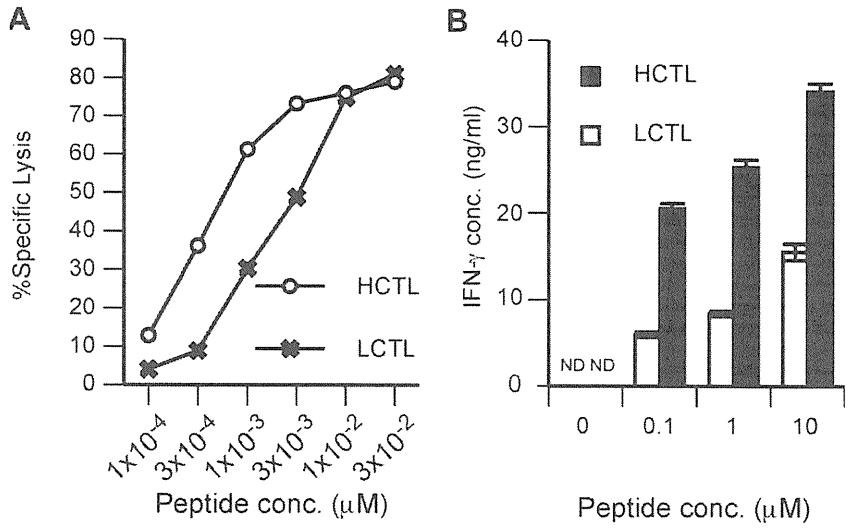

Fig. 2. Difference in functional avidity between HCTLs and LCTLs. (A) Recognition by the Tax11-19 peptide specific CTLs, HCTL and LCTL, of Tax11-19 antigenic peptide from 10^{-4} to 10 μM when presented on C1R.AAD target cells. The effector to target-cell (E/T) ratio was 20:1. Error bars were omitted because all SEMs were <3.5%. (B) Comparison of Tax11-19-specific IFN-γ production between HCTLs and LCTLs. A total of 200,000 CTL cells were cultured with 100,000 mytomicin-c treated C1R.AAD cell with 0.1–10 μM Tax11-19 peptide. Culture supernatants at 24 h were assayed using IFN-γ ELISA kit according to the manufacturer's instructions. ND, not detected.

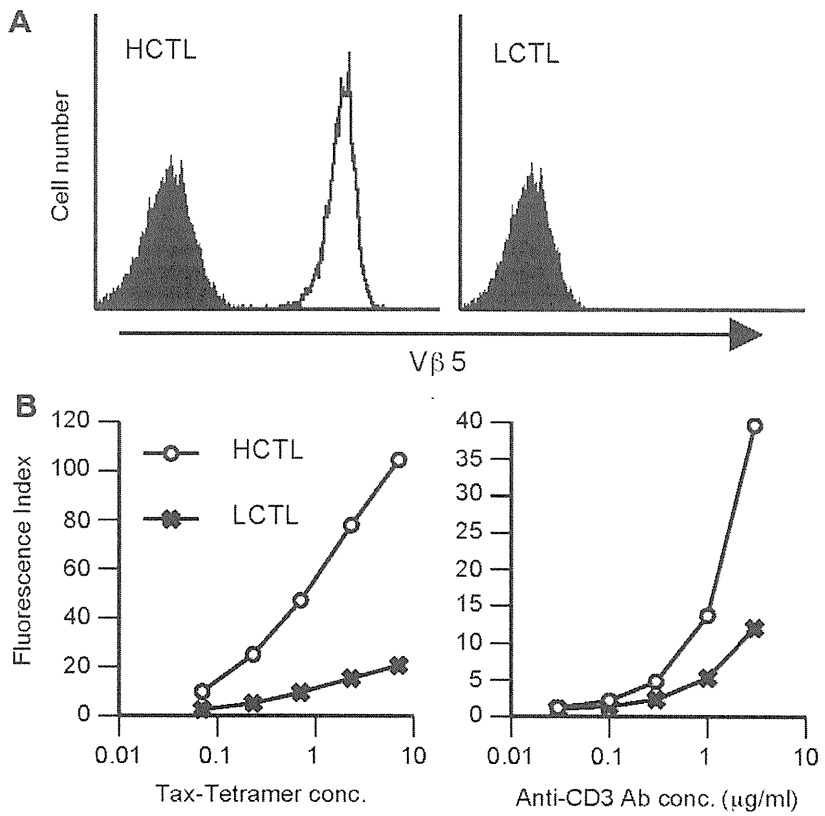

Fig. 3. TCR Vβ usage and expression level of TCR complex on Tax-specific CTLs with different functional avidity. (A) Comparison of Vβ usage pattern between HCTLs and LCTLs cytometry analysis (FCM). No Vβs among available anti-Vβ antibodies were detected in LCTL but only Vβ5 was detected in HCTL. (B) Comparison of binding curves for human Tax11-19-tetramer and anti-CD3ε Ab between HCTLs and LCTLs. HCTLs consistently showed a stronger fluorescence index than LCTLs; for Tax11-19-tetramer, the ratio of fluorescence index (LCTL/HCTL) was ~5-fold, and for anti-CD3ε Ab, it was ~3-fold.

3.5. Recognition of HTLV-1 infected human T cells by Tax-specific CTL from HHD mice

Next, in order to examine a comparison of the cytotoxicity against HTLV-1 infected non-tumor cells, we used HTLV-1 infected human T cells (HCT-4) derived from a patient with HAM/TSP [25]. On a 12 h lytic assay, HCTLs showed more efficient cytotoxicity against the HTLV-1 infected human T cells while LCTLs were not able to kill the targets under the these experimental conditions (Fig. 5A). At no time point was there detectable killing by LCTLs (Fig. 5B). These findings suggested that the superior recognition ability by the CTLs with higher functional avidity may have a more

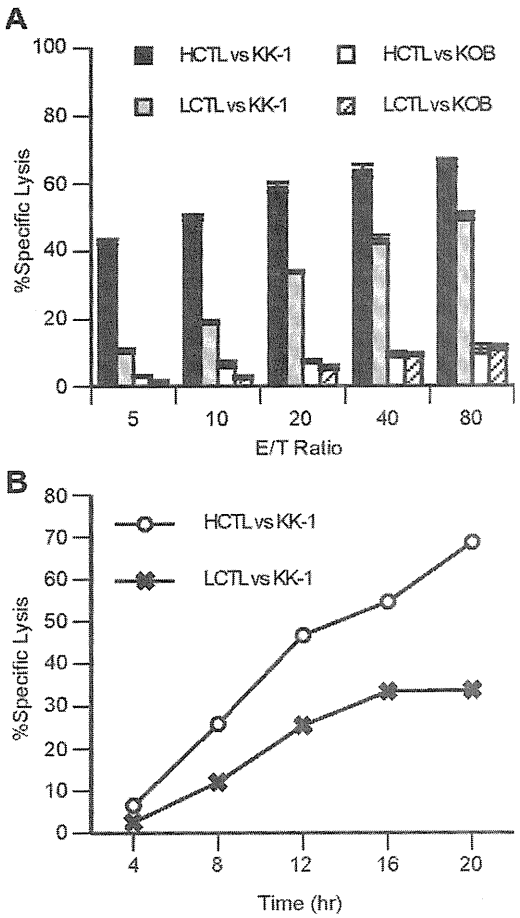

Fig. 4. Recognition pattern of human ATL targets by Tax-specific CTLs. (A) Comparison of cytotoxicity for human ATL targets (KK1, HLA-A2; KOB, HLA-A30) between HCTLs and LCTLs. (12 h ^{51}Cr release assay) (B) Comparison of kinetics of Tax-specific CTL-mediated cytotoxicity (E:T ratio = 40:1) between HCTLs and LCTLs. Similar results were obtained in three different experiments.

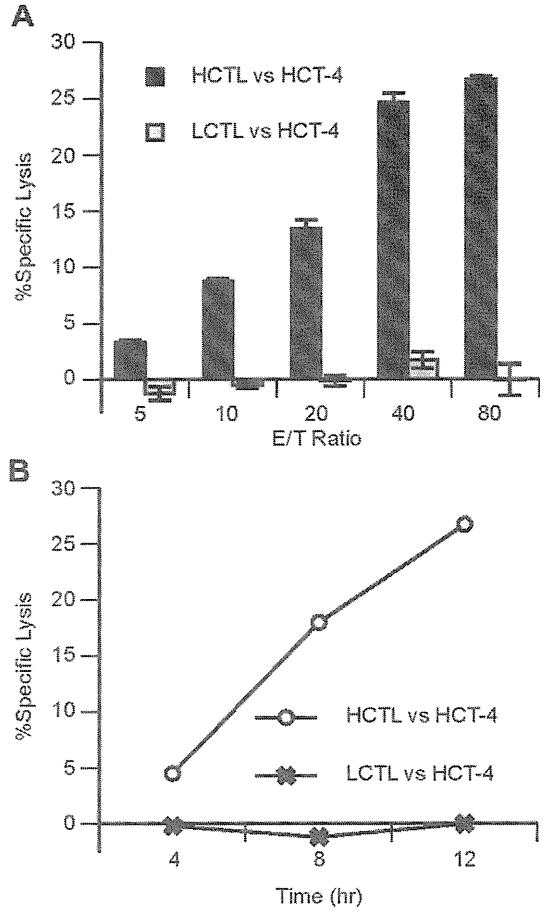

Fig. 5. Recognition pattern of HTLV-1 infected human T cell line by Tax-specific CTLs. (A) Comparison of cytotoxicity for human IL-2 dependent HTLV-1 infected cell, HCT-4 (HLA-A2), between HCTLs and LCTLs. (12 h ^{51}Cr release assay). (B) Comparison of kinetics of Tax-specific CTL-mediated cytotoxicity (E:T = 40:1) between HCTLs and LCTLs. Similar results were obtained in four different experiments.

striking effect in the case of recognizing normal cells infected with the virus.

3.6. Expression of Tax product in human ATL tumors and HTLV-1 infected T cell target

The cytotoxicity data against human targets indicated that higher functional avidity in CTLs is critical for efficient cytotoxicity against tumor or infected normal cell targets in humans. However, the amount of Tax antigen expressed in target cells that could be recognized by higher avidity CTLs was unclear. Therefore, we investigated how much Tax products could be yielded in these human ATL and HTLV-1 infected target cells. Using western blotting (Fig. 6A), Tax protein was detected in KOB and HCT-4 target cells, but not in KK-1. Since KK-1 cells were recognized by HCTLs more strongly than by LCTLs, we further evaluated the level of Tax mRNA produced in KK-1 using real-time PCR. The expression levels of Tax mRNA in KK-1 were around one thousand-fold lower than that in KOB (Fig. 6B). These results demonstrated that Tax11-19-specific higher avidity CTLs showed more efficient cytotoxicity against ATL by recognizing very small amount of Tax product detected only with real-time PCR.

4. Discussion

HTLV-1 infection elicits a strong CTL response, with Tax protein being the major target of HTLV-1-specific CTLs [10,11]. In the field of anti-tumor immunity, the in vivo relevance of differences in functional avidity has been established by demonstrating that high-avidity CTLs clear tumor antigens more efficiently than low-avidity CTL [34–38]. In HTLV-1 infection, however, while there is increasing body of evidence that CTL quality from the aspect of functional avidity of CTL might be crucial for the efficient control of HTLV-1 infection [17,39], little is known about how the functional avidity of HTLV-1 virus-specific CTLs is related to the control of HTLV-1-infected cells and tumors. Furthermore, the virus is latent in the tumor cells and it is difficult to detect expression of viral proteins [40–42]. This is the reason why there has not been direct evidence on whether Tax11-19 works as a definitive CTL antigen in HLA-A2-restricted patients with HTLV-1 infection and ATLs. The present study provides clear evidence regarding the notion that high avidity CTLs specific for Tax protein play a greater role in the specific destruction of ATL and HTLV-1-infected cells using Tax-specific CTLs with different functional avidity generated from HLA-A2 transgenic HHD mice, with human ATL lines and HTLV-1 infected cells acting as targets. As Tax11-19 peptide antigen binds HLA-A2 with almost as high affinity as FMP58-66 in influenza A virus (Fig. 1), which has one of the highest affinity peptides among HLA-A2 restricted peptide antigens [27,28], we developed CTL lines specific for Tax11-19, HCTL and LCTL, for which we found the optimum antigen-presenting conditions for the induction and maintenance of the CTL lines were 10 nM- and

10 μM-peptide pulsing APCs, respectively. The 1000-fold difference of such antigenic concentration resulted in the CTL lines with differences of functional avidity in antigen-specific cytotoxicity and IFN-γ production (Fig. 2). These different avidity CTLs also had different repertoires of TCRVβ, suggesting the structure of TCR in the major repertoire of two lines were distinct (Fig. 3A). In order to compare TCR affinity for the human Tax-tetramer, the mismatch of which to murine CD8 could permit assessment of the strength of TCR ligation to peptide/MHC complex more closely without the influence of CD8 binding [43], we titrated the tetramer and evaluated the effect of the number of TCR molecules expressed at the same time. Higher avidity Tax-specific CTLs showed higher fluorescene on both Tax-tetramer (~5-fold) and anti-CD3Ab (~3-fold) staining (Fig. 3B), thus suggesting that CTL might acquire higher avidity state by possessing the different structure of the TCR as well as by increasing the number of TCR molecules expressed although other factors could also play a role for determining the avidity of CTLs [15].

HTLV-1 Tax, a critical viral protein for HTLV-1 leukemogenesis, is the most likely target for HTLV-1 specific CTL in HTLV-1-infected individuals [10,11]. In HTLV-1-infected patients with HLA-A2, the Tax11-19-specific CTL response is predominantly detected in culture [44]. However, few details are known about the recognition mechanism by Tax-specific CTLs because of the difficulty of developing CTL lines specific for Tax11-19 antigen [9]. Although both HCTLs and LCTLs developed from HLA-A2 transgenic mice were not able to induce cytotoxicity against the human HLA-A2-restricted ATL line, KK-1, on 4 h assay because of the mismatch between the murine CD8 and human α3 domain [22], HCTLs clearly showed more efficient cytotoxicity than LCTLs with longer-term assay of more than 4 h (Fig. 4). Furthermore, the use of the human IL-2-dependent HTLV-1-infected non-tumor cell, HCT-4, clearly brought out the difference in cytotoxic efficacy between HCTL and LCTL (Fig. 5). These findings could be direct evidence not only that Tax11-19 might be naturally processed for presentation as a CTL antigen in both ATL tumor cells and virus-infected cells but also that the higher avidity CTL for Tax11-19 could be more critical in clearing HTLV-1-infected cells as well as ATL tumors in HLA-A2-restricted patients. In addition, HCTLs could more strongly recognize a latent level of Tax product detected only with a real-time PCR, not detectable with western blotting in the ATL target (Fig. 6). Furthermore, HCTLs also possessed higher elimination potential against HTLV-1 infected non-tumor targets when compared with LCTLs (Figs. 4 and 5).

The present findings are consistent with previous reports showing that the lytic efficiency of $CD8^+$ T cell response was inversely correlated with the proviral load and the rate of proviral expression in patients with HTLV-1 infection [17]. These data also strongly support the notion that induction of high avidity CTLs is critical for development of more effective vaccines against cancer and chronic viral infection such as HTLV-1and HIV. In addition, based on the observation that the high-avidity CTLs expressed a greater number of TCR molecules when compared with the low-avidity CTLs (Fig. 3B), such more multivalent TCR display might be one of the critical factors in establishing functional high avidity, leading to more efficient TCR cell therapy in the future [45].

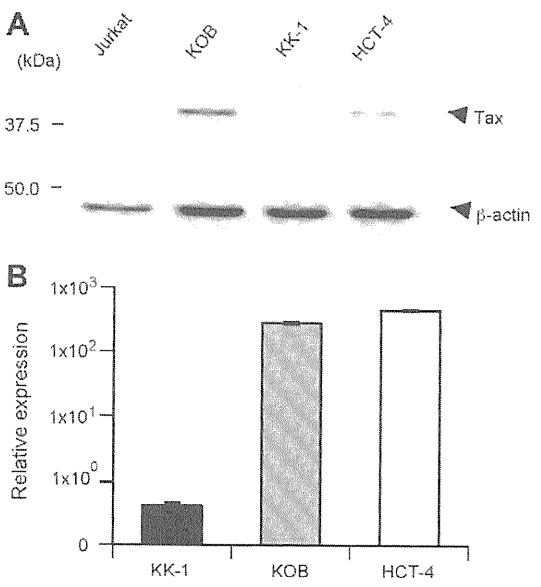

Fig. 6. Expression of Tax product in human ATL tumors and HTLV-1 infected T cell targets. (A) Tax protein is detected in KOB and HCT-4 by western blotting, but not in KK-1. Jurkat cells were used as a negative control. (B) Comparison of mRNA production of Tax by real-time PCR among KOB, KK-1 and HCT-4. Tax production in KK-1 was detected by real-time PCR, but not in a western blotting. Jurkat cells as a negative control gave no detectable signal with the Tax-primer.

Conflict of interest

The authors declare no conflict of interest.

Acknowledgments

We would like to thank Dr. Jay A. Berzofsky for critical reading of the manuscript and helpful suggestions. We also would like to thank Hiroe Ogasawara and Katsunori Takahashi for technical assistance provided during the study.

References

[1] Y. Hinuma, K. Nagata, M. Hanaoka, M. Nakai, T. Matsumoto, K.I. Kinoshita, S. Shirakawa, I. Miyoshi, Adult T-cell leukemia: antigen in an ATL cell line and detection of antibodies to the antigen in human sera, Proc. Natl. Acad. Sci. USA 78 (1981) 6476–6480.
[2] M. Yoshida, M. Seiki, K. Yamaguchi, K. Takatsuki, Monoclonal integration of human T-cell leukemia provirus in all primary tumors of adult T-cell leukemia suggests causative role of human T-cell leukemia virus in the disease, Proc. Natl. Acad. Sci. USA 81 (1984) 2534–2537.
[3] A. Gessain, F. Barin, J.C. Vernant, O. Gout, L. Maurs, A. Calender, G. De The, Antibodies to human T-lymphotropic virus type-I in patients with tropical spastic paraparesis, Lancet 2 (1985) 407–410.
[4] M. Osame, K. Usuku, S. Izumo, N. Ijichi, H. Amitani, A. Igata, M. Matsumoto, M. Tara, HTLV-I associated myelopathy, a new clinical entity, Lancet 1 (1986) 1031–1032.
[5] T. Matsuzaki, M. Nakagawa, M. Nagai, K. Usuku, I. Higuchi, K. Arimura, H. Kubota, S. Izumo, S. Akiba, M. Osame, HTLV-I proviral load correlates with progression of motor disability in HAM/TSP: analysis of 239 HAM/TSP patients including 64 patients followed up for 10 years, J. Neurovirol. 7 (2001) 228–234.
[6] M.A. Nowak, C.R. Bangham, Population dynamics of immune responses to persistent viruses, Science 272 (1996) 74–79.
[7] A.M. Vine, A.G. Heaps, L. Kaftantzi, A. Mosley, B. Asquith, A. Witkover, G. Thompson, M. Saito, P.K. Goon, L. Carr, F. Martinez-Murillo, G.P. Taylor, C.R. Bangham, The role of CTLs in persistent viral infection: cytolytic gene expression in CD8+ lymphocytes distinguishes between individuals with a high or low proviral load of human T cell lymphotropic virus type 1, J. Immunol. 173 (2004) 5121–5129.
[8] M. Kannagi, K. Sugamura, K. Kinoshita, H. Uchino, Y. Hinuma, Specific cytolysis of fresh tumor cells by an autologous killer T cell line derived from an adult T cell leukemia/lymphoma patient, J. Immunol. 133 (1984) 1037–1041.
[9] B. Arnulf, M. Thorel, Y. Poirot, R. Tamousa, E. Boulanger, A. Jaccard, E. Oksenhendler, O. Hermine, C. Pique, Loss of the ex vivo but not the reinducible CD8+ T-cell response to Tax in human T-cell leukemia virus type 1-infected patients with adult T-cell leukemia/lymphoma, Leukemia 18 (2004) 126–132.
[10] S. Jacobson, H. Shida, D.E. McFarlin, A.S. Fauci, S. Koenig, Circulating CD8+ cytotoxic T lymphocytes specific for HTLV-I pX in patients with HTLV-I associated neurological disease, Nature 348 (1990) 245–248.
[11] M. Kannagi, S. Harada, I. Maruyama, H. Inoko, H. Igarashi, G. Kuwashima, S. Sato, M. Morita, M. Kidokoro, M. Shigemoto, Predominant recognition of human T cell leukemia virus type I (HTLV-I) pX gene products by human CD8+ cytotoxic T cells directed against HTLV-I-infected cells, Int. Immunol. 3 (1991) 761–767.

[12] K.T. Jeang, Functional activities of the human T-cell leukemia virus type I Tax oncoprotein: cellular signaling through NF-kappa B, Cytokine Growth Factor Rev. 12 (2001) 207–217.
[13] M. Yoshida, Multiple viral strategies of HTLV-1 for dysregulation of cell growth control, Annu. Rev. Immunol. 19 (2001) 475–496.
[14] M. Kannagi, S. Matsushita, S. Harada, Expression of the target antigen for cytotoxic T lymphocytes on adult T-cell-leukemia cells, Int. J. Cancer 54 (1993) 582–588.
[15] M.A. Alexander-Miller, High-avidity CD8+ T cells: optimal soldiers in the war against viruses and tumors, Immunol. Res. 31 (2005) 13–24.
[16] M. Derby, M. Alexander-Miller, R. Tse, J.A. Berzofsky, High-avidity CTL exploit two complementary mechanisms to provide better protection against viral infection than low-avidity CTL, J. Immunol. 166 (2001) 1690–1697.
[17] T. Kattan, A. MacNamara, A.G. Rowan, et al., The avidity and lytic efficiency of the CTL response to HTLV-1, J. Immunol. 182 (9) (2009) 5723–5729.
[18] A. Gallimore, T. Dumrese, H. Hengartner, R.M. Zinkernagel, H.G. Rammensee, Protective immunity does not correlate with the hierarchy of virus-specific cytotoxic T cell responses to naturally processed peptides, J. Exp. Med. 187 (1998) 1647–1657.
[19] A.G. Cawthon, H. Lu, M.A. Alexander-Miller, Peptide requirement for CTL activation reflects the sensitivity to CD3 engagement: correlation with CD8ab versus CD8aa expression, J. Immunol. 167 (2001) 2577–2584.
[20] S. Walter, L. Herrgen, O. Schoor, G. Jung, D. Wernet, H.J. Buhring, H.G. Rammensee, S. Stevanovic, Cutting edge: predetermined avidity of human CD8 T cells expanded on calibrated MHC/anti-CD28-coated microspheres, J. Immunol. 171 (2003) 4974–4978.
[21] P.M. Gray, G.D. Parks, M.A. Alexander-Miller, High avidity CD8+ T cells are the initial population elicited following viral infection of the respiratory tract, J. Immunol. 170 (2003) 174–181.
[22] M.H. Newberg, D.H. Smith, S.B. Haertel, D.R. Vining, E. Lacy, V.H. Engelhard, Importance of MHC class 1 a2 and a3 domains in the recognition of self and non-self MHC molecules, J. Immunol. 156 (1996) 2473–2480.
[23] Y. Yamada, Y. Nagata, S. Kamihira, M. Tagawa, M. Ichimaru, M. Tomonaga, H. Shiku, IL-2-dependent ATL cell lines with phenotypes differing from the original leukemia cells, Leuk. Res. 15 (1991) 619–625.
[24] T. Maeda, Y. Yamada, R. Moriuchi, K. Sugahara, K. Tsuruda, T. Joh, S. Atogami, K. Tsukasaki, M. Tomonaga, S. Kamihara, Fas gene mutation in the progression of adult T cell leukemia, J. Exp. Med. 189 (1999) 1063–1071.
[25] N. Fukushima, Y. Nishiura, T. Nakamura, Y. Yamada, S. Kohno, K. Eguchi, Involvement of p38 MAPK signaling pathway in IFN-g and HTLV-I expression in patients with HTLV-I-associated myelopathy/tropical spastic paraparesis, J. Neuroimmunol. 159 (2005) 196–202.
[26] S. Pascolo, N. Bervas, J.M. Ure, A.G. Smith, F.A. Lemonnier, B. Perarnau, HLA-A2.1-restricted education and cytolytic activity of CD8(+) T lymphocytes from b2 microglobulin (b2m) HLA-A2.1 monochain transgenic H-2Db b2m double knockout mice, J. Exp. Med. 185 (1997) 2043–2051.
[27] T. Okazaki, C.D. Pendleton, F. Lemonnier, J.A. Berzofsky, Epitope-enhanced conserved HIV-1 peptide protects HLA-A2-transgenic mice against virus expressing HIV-1 antigen, J. Immunol. 171 (2003) 2548–2555.
[28] T. Okazaki, M. Terabe, A.T. Catanzaro, C.D. Pendleton, R. Yarchoan, J.A. Berzofsky, Possible therapeutic vaccine strategy against human immunodeficiency virus escape from reverse transcriptase inhibitors studied in HLA-A2 transgenic mice, J. Virol. 80 (2006) 10645–10651.
[29] A. Maeda, T. Okazaki, M. Inoue, T. Kitazono, M. Yamasaki, F.A. Lemonnier, S. Ozaki, Immunosuppressive effect of angiotensin receptor blocker on stimulation of mice CTLs by angiotensin II, Int. Immunopharmacol. 9 (2009) 1183–1188.
[30] B. Lee, Y. Tanaka, H. Tozawa, Monoclonal antibody defining tax protein of human T-cell leukemia virus type-I, Tohoku J. Exp. Med. 157 (1989) 1–11.
[31] Y. Yamano, N. Araya, T. Sato, A. Utsunomiya, K. Azakami, D. Hasegawa, T. Izumi, H. Fujita, S. Aratani, N. Yagishita, R. Fujii, K. Nishioka, S. Jacobson, T. Nakajima, Abnormally high levels of virus-infected IFN-g+ CCR4+ CD4+ CD25+ T cells in a retrovirus-associated neuroinflammatory disorder, PLoS ONE 4 (2009) e6517.
[32] F. Gotch, J. Rothbard, K. Howland, A. Townsend, A. McMichael, Cytotoxic T lymphocytes recognize a fragment of influenza virus matrix protein in association with HLA-A2, Nature 326 (1987) 881–882.
[33] M.H. Newberg, J.P. Ridge, D.R. Vining, R.D. Salter, V.H. Engelhard, Species specificity in the interaction of CD8 with the a3 domain of MHC class I molecules, J. Immunol. 149 (1992) 136–142.
[34] M.A. Alexander-Miller, G.R. Leggatt, J.A. Berzofsky, Selective expansion of high- or low-avidity cytotoxic T lymphocytes and efficacy for adoptive immunotherapy, Proc. Natl. Acad. Sci. USA 93 (1996) 4102–4107.
[35] C. Sedlik, G. Dadaglio, M.F. Saron, E. Deriaud, M. Rojas, S.I. Casal, C. Leclerc, In vivo induction of a high-avidity, high-frequency cytotoxic T-lymphocyte response is associated with antiviral protective immunity, J. Virol. 74 (2000) 5769–5775.
[36] V. Dutoit, V. Rubio-Godoy, P.Y. Dietrich, A.L. Quiqueres, V. Svhnuriger, D. Rimoldi, D. Lienard, D. Speiser, P. Guillaume, P. Batard, J.C. Cerottini, P. Romero, D. Valmori, Heterogeneous T-cell response to MAGE-A10(254–262): high avidity-specific cytolytic T lymphocytes show superior antitumor activity, Cancer Res. 61 (2001) 5850–5856.
[37] C. Yee, P.A. Savage, P.P. Lee, M.M. Davis, P.D. Greenberg, Isolation of high avidity melanoma-reactive CTL from heterogeneous populations using peptide-MHC tetramers, J. Immunol. 162 (1999) 2227–2234.
[38] H.J. Zeh III, D. Perry-Lalley, M.E. Dudley, S.A. Rosenberg, J.C. Yang, High avidity CTLs for two self-antigens demonstrate superior in vitro and in vivo antitumor efficacy, J. Immunol. 162 (1999) 989–994.
[39] C.R. Bangham, CTL quality and the control of human retroviral infections, Eur. J. Immunol. 39 (2009) 1700–1712.
[40] H. Konishi, N. Kobayashi, M. Hatanaka, Defective human T-cell leukemia virus in adult T-cell leukemia patients, Mol. Biol. Med. 2 (1984) 273–283.
[41] T. Kinoshita, M. Shimoyama, K. Tobinai, M. Ito, S. Ito, S. Ikeda, K. Tajima, K. Shimotohno, T. Sugimura, Detection of mRNA for the tax1/rex1 gene of human T-cell leukemia virus type I in fresh peripheral blood mononuclear cells of adult T-cell leukemia patients and viral carriers by using the polymerase chain reaction, Proc. Natl. Acad. Sci. USA 86 (1989) 5620–5624.
[42] T. Uchiyama, Human T cell leukemia virus type I (HTLV-I) and human diseases, Annu. Rev. Immunol. 15 (1997) 15–37.
[43] E.M. Choi, J.L. Chen, L. Wooldridge, M. Salio, A. Lissina, N. Lissin, I.F. Hermans, J.D. Silk, F. Milza, M.J. Palmowski, P.R. Dumbar, B.K. Jacobson, A.K. Sewell, V. Cerundolo, High avidity antigen-specific CTL identified by CD8-independent tetramer staining, J. Immunol. 171 (2003) 5116–5123.
[44] M. Kannagi, H. Shida, H. Igarashi, K. Kuruma, H. Murai, Y. Aono, I. Maruyama, M. Osame, T. Hattori, H. Inoko, Target epitope in the Tax protein of human T-cell leukemia virus type I recognized by class I major histocompatibility complex-restricted cytotoxic T cells, J. Virol. 66 (1992) 2928–2933.
[45] C. Govers, Z. Sebestyen, M. Coccoris, R.A. Willemsen, R. Debets, T cell receptor gene therapy: strategies for optimizing transgenic TCR pairing, Trends Mol. Med. 16 (2010) 77–87.

J. Biochem. 2011;150(6):679–686 doi:10.1093/jb/mvr106

THE JOURNAL OF BIOCHEMISTRY

Activation of the IκB kinase complex by HTLV-1 Tax requires cytosolic factors involved in Tax-induced polyubiquitination

Received August 3, 2011; accepted August 13, 2011; published online August 23, 2011

Yuri Shibata[1], Yuetsu Tanaka[2], Jin Gohda[1] and Jun-ichiro Inoue[1,*]

[1]Department of Cancer Biology, Division of Cellular and Molecular Biology, Institute of Medical Science, University of Tokyo, Shirokane-dai, Minato-ku, Tokyo 108-8639; and [2]Department of Immunology, Faculty of Medicine, University of the Ryukyus, Nishihara, Okinawa 903-0213, Japan

*Jun-ichiro Inoue, Department of Cancer Biology, Division of Cellular and Molecular Biology, Institute of Medical Science, University of Tokyo, 4-6-1 Shirokane-dai, Minato-ku, Tokyo 108-8639, Japan. Tel: +81 3 5449 5275, Fax: +81 3 5449 5421, email: jun-i@ims.u-tokyo.ac.jp

Activation of NF-κB by human T cell leukaemia virus type 1 Tax is thought to be crucial in T-cell transformation and the onset of adult T cell leukaemia. Tax activates NF-κB through activation of the IκB kinase (IKK) complex, similar to cytokine-induced NF-κB activation, which involves active signalling complex formation using polyubiquitin chains as a platform. Although polyubiquitination of Tax was reported to be required for IKK activation, most studies have been performed using intact cells, in which secondary NF-κB activation can be induced by various cytokines that are secreted due to Tax-mediated primary NF-κB activation. Therefore, a cell-free assay system, in which IKK can be activated by adding highly purified recombinant Tax to cytosolic extract, was used to analyse Tax-induced IKK activation. In contrast to the cytosolic extract, the purified IKK complex was not activated by Tax, whereas, it was efficiently activated by MEKK1, that does not require polyubiquitination to activate IKK. Moreover, Tax-induced IKK activation was blocked when the cytosolic extract was mixed with either lysine-free, methylated or K63R ubiquitin. These results obtained through our cell-free assay suggest that K63-linked polyubiquitination is critical, but linear polyubiquitination is dispensable or insufficient for Tax-induced IKK activation.

Keywords: Human T cell leukaemia virus type 1/IκB kinase/NF-κB/polyubiquitination/Tax.

Abbreviations: ATL, Adult T-cell leukaemia; CYLD, cylindromatosis; HTLV-1, Human T cell leukaemia virus type 1; IKK, IκB kinase; MEKK1, MAPK/ERK kinase; NEMO, NF-κB essential modulator; NF-κB, nuclear factor-κB; TRAF6, TNF receptor-associated factor 6.

Human T-cell leukaemia virus type 1 (HTLV-1) infects and transforms $CD4^+$ T cells *in vitro* and is etiologically associated with an acute T cell malignancy, Adult T-cell leukaemia (ATL) (*1*). The HTLV-1 genome encodes the Tax protein, which plays a critical role in T-cell transformation (*2*, *3*). Tax regulates the expression of cellular genes involved in T-cell proliferation, cell survival and anti-apoptosis by modulating various transcription factors, including nuclear factor-κB (NF-κB), cAMP-responsible element binding protein (CREB) and serum response factor (SRF) (*1*, *4*). NF-κB is one of the key transcription factors that facilitate cell transformation because the Tax mutant M22, which can activate CREB but not NF-κB, is unable to immortalize T cells (*5*). Therefore, elucidation of the mechanism that underlies Tax-induced NF-κB activation may aid in preventing the onset of ATL.

NF-κB is normally sequestered in the cytoplasm by associating with inhibitory proteins from the NF-κB family (IκBs). Extracellular stimuli, such as tumour necrosis factor (TNF)-α and interleukin (IL)-1, activate the IκB kinase (IKK) complex, that is composed of the catalytic subunits IKKα and IKKβ and the regulatory subunit NF-κB essential modulator (NEMO). The activated IKK complex phosphorylates IκBα, which, in turn, induces Lys48-linked polyubiquitination and proteasomal degradation of IκBα. NF-κB is then translocated into the nucleus and promotes transcription of its target genes (*6*). It has been well established that Lys63-linked polyubiquitination is involved in the cytokine-mediated NF-κB activation pathway (*7*). In the interleukin-1 receptor (IL-1R) and Toll-like receptor (TLR) signalling pathways, TNF receptor (TNFR)-associated factor 6 (TRAF6), an E3 ubiquitin ligase, conjugates Lys63-linked polyubiquitination to itself and TGF-β-activated kinase (TAK) 1 together with Ubc13, an E2 ubiquitin-conjugating enzyme (*8*, *9*). Polyubiquitination leads to formation of a signalling complex that contains MAPK/ERK kinase (MEKK3), TAK1, TAK1-binding (TAB) 2/TAB3 and the IKK complex, which induces activation of TAK1 and the IKK complex (*10*). In TNFR1 signalling, cIAPs act as an E3 ubiquitin ligase that conjugates polyubiquitin chains to receptor-interacting protein (RIP) 1 (*11*, *12*). Polyubiquitin chains that are conjugated to RIP1 also act as platforms for the formation of a signalling complex to activate downstream molecules.

To date, many studies have been conducted to elucidate the mechanism of Tax-induced IKK activation. Tax binds to NEMO and induces activation of the IKK complex (*13*, *14*). We have shown that, unlike the cytokine-mediated NF-κB signalling pathway, Tax does not require Ubc13 and MAP3Ks, including TAK1, MEKK1, MEKK3, NF-κB-inducing kinase (NIK) and tumor progression locus (TPL)-2 for IKK

activation (*15*). We have further shown that expression of cylindromatosis (CYLD) does not affect Tax-induced NF-κB activation, whereas it does inhibit TRAF6-induced NF-κB activation (*15*), which led us to hypothesize that polyubiquitination may not be required for Tax-induced NF-κB activation. However, other groups have shown that Ubc13 and TAK1 are required for Tax-induced NF-kB activation (*16*). Therefore, the molecular mechanisms for Tax-induced IKK activation are controversial and largely unknown.

Herein, we establish a cell-free assay system that induces IKK activation in response to recombinant Tax and demonstrate that Tax requires unidentified cytosolic factor(s) to activate the purified IKK complex. We further show that a ubiquitin mutant, which is unable to form polyubiquitin chains, inhibit activation of the IKK complex, which suggests that polyubiquitination is involved in the Tax-induced IKK activation pathway.

Experimental Procedures

Plasmids

The cDNAs that encode Tax, M22, TRAF6, MEKK1 (the C-terminal 321 amino acids) were inserted into the pFastBac^{TM} HT A vector (Invitrogen) to generate a recombinant baculovirus for expression of these proteins in Sf9 cells.

Cell culture and reagents

The Jurkat and JM4.5.2 cells were maintained in RPMI 1640 with 10% heat-inactivated fetal bovine serum (FBS). The Sf9 cells were maintained in Sf900^{TM} II SFM (Gibco) with 10% heat-inactivated FBS. Wild-type (WT) and *Traf6*$^{-/-}$ mouse embryonic fibroblasts (MEFs) (*17*) were maintained in Dulbecco's modified Eagle's medium (DMEM) with 10% heat-inactivated FBS. BAY 11-7082 and BMS-345541 were obtained from Calbiochem. The wild-type ubiquitin and ubiquitin mutants were purchased from Boston Biochem.

Purification of the recombinant proteins

His_6-tagged Tax, M22, TRAF6 and MEKK1 were produced using the Bac-to-Bac Baculovirus Expression System (Invitrogen). Briefly, a 50-ml culture of Sf9 cells (1×10^6 cells/ml) was infected with a recombinant baculovirus that expressed each protein. On completing 72 h after infection, the cells were harvested, and the His_6-tagged recombinant proteins were purified using the Ni-NTA resin (QIAGEN) according to the manufacturer's instructions.

Preparation of cytosolic extract (S100) from Jurkat cells

The Jurkat cells (1.5×10^8 cells) were resuspended in 500 μl of hypotonic buffer [10 mM Tris–HCl (pH 7.5), 1.5 mM $MgCl_2$, 10 mM KCl, 0.5 mM dithiothreitol (DTT) and a protease inhibitor cocktail (Roche)] and homogenized using a Dounce homogenizer. The cell debris was removed by ultracentrifugation at 100,000*g* for 1 h, and the cleared supernatant (S100) was collected.

Cell-free assay for IKK activation

The Jurkat cytosolic extract (10 mg/ml) was incubated with the indicated amount of either recombinant Tax, M22, TRAF6 or MEKK1 in ATP buffer [50 mM Tris–HCl (pH 7.5), 5 mM $MgCl_2$, 2 mM ATP, 5 mM NaF, 20 mM β-glycerophosphate, 1 mM Na_3VO_4 and a protease inhibitor cocktail]. After incubation at 30°C for 1 h, the reaction mixtures were immunoblotted, immunoprecipitated or pulled down. For the cell-free assay using the purified IKK complex, the IKK complex was immunoprecipitated with an anti-Flag antibody from Jurkat cells that stably expressed Flag-NEMO (5.0×10^8 cells). The purified IKK complex was incubated with the indicated recombinant proteins in the presence of 100 ng of GST-IκBα (amino acids 1–54) in ATP buffer.

Immunoblotting

Either the immunoprecipitates or the whole-cell lysates were separated by sodium dodecyl sulfate–polyacrylamide gel electrophoresis (SDS–PAGE) and transferred to a polyvinylidenedifluoride (PVDF) membrane (Millipore). The membranes were incubated with the appropriate primary antibodies. Immunoreactive proteins were visualized with anti-rabbit or anti-mouse IgG conjugated to horseradish peroxidase (Amersham Biosciences), followed by processing with an enhanced chemiluminescence (ECL) detection system (Amersham Biosciences). The following antibodies were used: anti-p-IκBα (9246), anti-IκBα (9242), anti-p-IKKα/IKKβ (2681), anti-IKKα (2682), anti-IKKβ (2684) and anti-NEMO (2695) from Cell Signaling Technology as well as ubiquitin (sc-8017) (Santa Cruz Biotechnology), anti-Tubulin (CP06) (Calbiochem), anti-His-tag (PM032) (MBL) and anti-Tax (Lt-4).

Pull-down assay and immunoprecipitation

For the pull-down assays, pull down buffer [10 mM Tris–HCl [pH 7.0], 150 mM NaCl, 0.5 mM ethylenediaminetetraacetic acid (EDTA), 1% NP-40, 10 mM imidazole] and Ni-NTA resin were added to an *in vitro* assay reaction mixture. After incubation at 4°C for 1 h, the Ni-NTA resin was washed three times with the pull-down buffer and immunoblotted. To detect polyubiquitination of Tax and NEMO, the reaction mixtures were boiled for 10 min with 1% SDS to remove non-covalently attached proteins. The reaction mixtures were diluted 10-fold in Tris/NaCl/EDTA (TNE) buffer [20 mM Tris–HCl (pH 7.5), 150 mM NaCl, 2 mM EDTA, 1% NP-40, 5 mM *N*-ethylmaleimide and a protease inhibitor cocktail] to reduce the concentration of SDS to 0.1%. The reaction mixtures were then incubated with antibodies against Tax or NEMO. The immunoprecipitates were washed three times with TNE buffer and immunoblotted using an anti-Ub antibody.

Results and Discussion

Establishment of a cell-free assay system that reproduces Tax-induced IKK complex activation

Once Tax activates NF-κB, various cytokines, including TNF-α and IL-1, may be induced by NF-κB and secreted, which in turn further activates NF-κB through the cytokine-specific receptors on the Tax-expressing cells (*18*, *19*). This potential autocrine-stimulated NF-κB activation enhances the difficulty of distinguishing signalling events induced by Tax from those induced by cytokines. Therefore, we tried to establish an *in vitro* cell-free system, in which Tax-induced IKK activation can be analysed without cytokine-induced IKK activation. The involvement of polyubiquitination in Tax-induced IKK activation is unclear, although its involvement in cytokine-induced IKK activation has been established (*7*). Thus, the cell-free system is suitable to address the role of polyubiquitin chains in Tax-induced IKK activation. We first expressed recombinant His_6-Tax and the Tax mutant M22, which is defective in NF-κB activation, in Sf9 cells and purified them using Ni-NTA agarose (Fig. 1A) To examine whether recombinant Tax activates the IKK complex, the cytosolic extract was prepared from the human T cell line Jurkat and incubated with either recombinant Tax or M22, and the resulting reaction mixture was analysed using immunoblots with anti-p-IκBα and anti-p-IKKα/β antibodies. Recombinant Tax, but not recombinant M22, induced phosphorylation of IκBα in a dose-dependent manner (Fig. 1B). Phosphorylation of IκBα was also indicated by the appearance of a slower migrating form of IκBα (Fig. 1B). Phosphorylation of IKKα/β was also

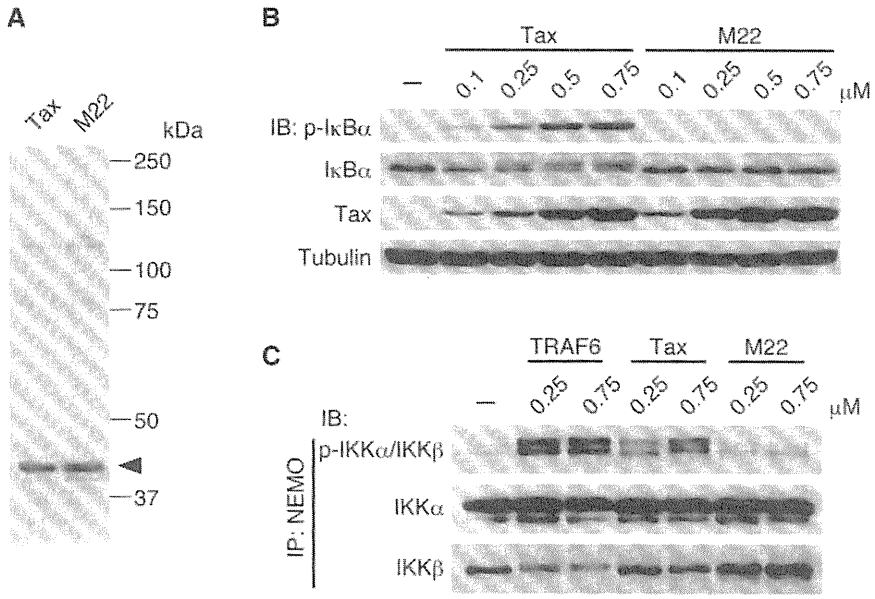

Fig. 1 Recombinant Tax activates the IKK complex in the cell-free assay system. (A) Purification of recombinant His_6-Tax and the Tax M22 mutant. We performed SDS–PAGE on the recombinant Tax and M22 that were purified from Sf9 cells, which was followed by silver staining. An arrow indicates the Tax protein. (B) Recombinant Tax induces phosphorylation of IκBα in a dose-dependent manner. The Jurkat cytosolic extract (10 mg/ml) was incubated with the indicated amount of recombinant either Tax or M22 with ATP (2 mM) at 30°C for 1 h. Phosphorylation of IκBα was detected by immunoblot with the anti-p-IκBα, anti-IκBα, anti-Tax and anti-Tubulin antibodies. (C) Recombinant Tax induces phosphorylation of the IKK complex. The Jurkat cytosolic extract (10 mg/ml) was incubated with the indicated amount of recombinant TRAF6, Tax or M22 at 30°C for 1 h. The reaction mixtures were immunoprecipitated with an anti-NEMO antibody and then immunoblotted with anti-p-IKKα/IKKβ, anti-IKKα and anti-IKKβ antibodies.

induced by recombinant Tax, but not by M22, to a similar extent as induced by TRAF6 (Fig. 1C).

To further confirm that recombinant Tax-induced phosphorylation of IκBα is catalysed by IKK, two distinct IKK inhibitors, BAY 11-7082 (*20*) and BMS-345541 (*21*), were added to the cell-free IKK activation system. Both of the IKK inhibitors inhibited Tax-induced phosphorylation of IκBα in a dose-dependent manner (Fig. 2A and B). Moreover, we performed the cell-free assay using cytosolic extract prepared from JM4.5.2, which is a NEMO-deficient Jurkat cell line, because the interaction of Tax with NEMO is indispensable to Tax-induced IKK activation (*22*, *23*). We confirmed that NEMO was not expressed in JM4.5.2 cells, whereas, IKKα and IKKβ were expressed to a similar extent in the JM4.5.2 and Jurkat cells (Fig. 2C, left). Previous study has shown that TRAF6 fails to induce IκBα phosphorylation in the absence of NEMO (*9*). While we reproduced the TRAF6 requirement for NEMO, recombinant Tax also failed to induce IκBα phosphorylation in the NEMO-deficient cytosolic extract (Fig. 2C, right). To examine whether Tax binding to the IKK complex depends on NEMO in the cell-free assay, Tax was pulled down with Ni-NTA beads, and IKKα/β binding to Tax was analysed by immunoblots. Recombinant Tax interacted with the IKK complex in the Jurkat cytosolic extract, whereas, Tax did not bind the IKK complex without NEMO (Fig. 2D). Taken together, Tax binds the IKK complex through NEMO and subsequently activates the IKK complex in the cell-free assay system. Given that M22, which is unable to bind NEMO (*14*), does not activate the IKK complex in the cell-free system (Fig. 1B and C), these results strongly suggest that our cell-free assay system reconstitutes the Tax-mediated NF-κB activation in intact cells. A similar assay system has been reported previously using partially purified recombinant Tax generated in *Escherichia coli* (*24*). As the purity of our Tax protein generated in sf9 cells is >95% (Fig. 1A) and its specific activity may be >8-fold over that of the Tax from *E. coli* [a minimum concentration of the Tax from Sf9 required for IKK activation is ~0.1 μM (Fig. 1B) while that of the Tax from *E. coli* is ~0.8 μM (*24*)], our system is well suited for further investigation of the molecular mechanism for Tax activation of NF-κB.

Tax requires cytosolic intermediary factors for activation of the purified IKK complex

Using the cell-free systems, we next addressed whether Tax alone induces IKK activation. The IKK complex was purified from unstimulated Jurkat cells and then incubated with either recombinant Tax or other NF-κB activators and recombinant GST-IκBα. As MEKK1 alone is known to activate the purified IKK complex without the polyubiquitination reaction (*9*, *25*), we used MEKK1 as a positive control. On the other hand, TRAF6 requires other molecules, such as Ubc13, Uev1a, TAK1 and TAB2, for IKK activation (*9*, *26*). Therefore, TRAF6 was used as a negative control. When incubated with Jurkat cytosolic extracts, all the recombinant proteins were able to induce phosphorylation of IκBα (Fig. 3A). However, when the recombinant proteins were incubated with the purified IKK complex, only MEKK1 induced phosphorylation of IκBα and IKKβ (Fig. 3B, +IKK).

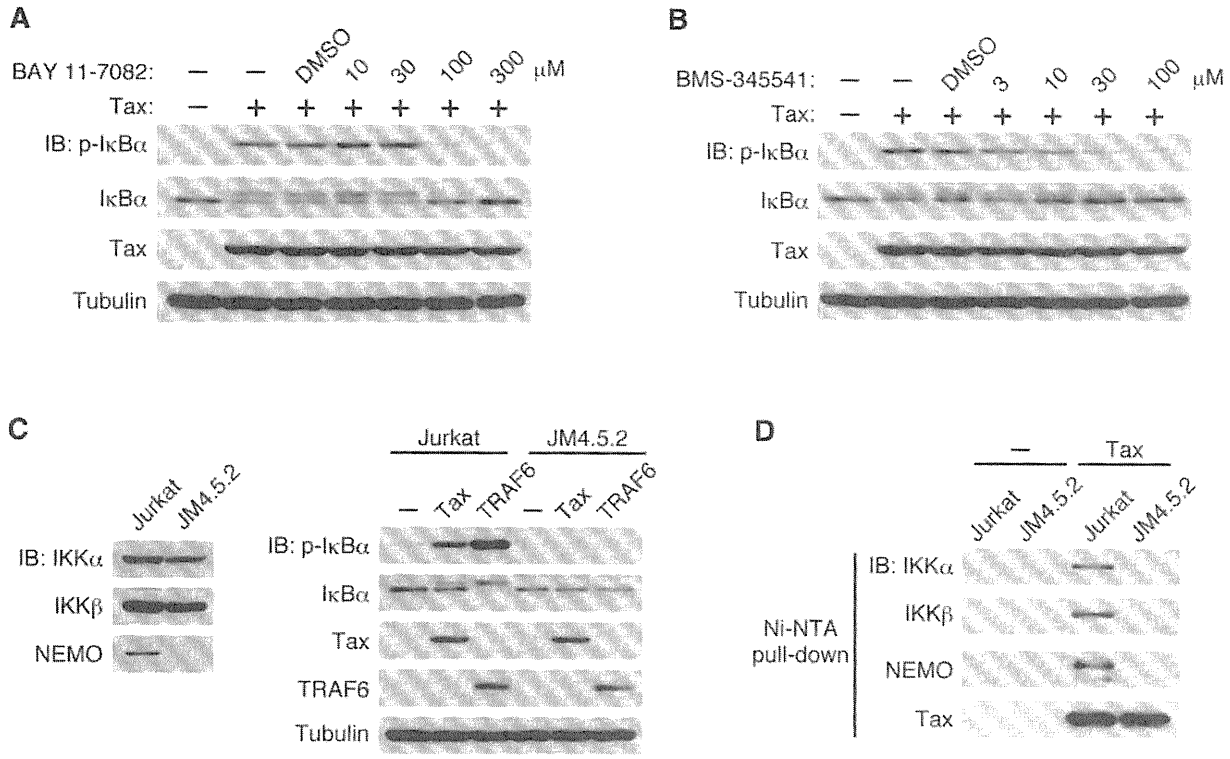

Fig. 2 Phosphorylation of IκBα induced by recombinant Tax is dependent on IKK activation. (A and B) IKK inhibitors inhibit IκBα phosphorylation induced by recombinant Tax in a dose-dependent manner. The Jurkat cytosolic extract (10 mg/ml) was incubated with recombinant Tax (0.5 μM) and ATP (2 mM) and either the IKK inhibitor BAY 11-7082 (A) or BMS-345541 (B) at 30°C for 1 h. Phosphorylation of IκBα was detected by immunoblot with an anti-p-IκBα antibody. (C) NEMO is essential for Tax-induced phosphorylation of IκBα. The expression levels of IKKα, IKKβ and NEMO were analysed by immunoblot (left). Either the Jurkat or JM4.5.2 cytosolic extract (10 mg/ml) was incubated with either recombinant TRAF6 (0.5 μM) or Tax (0.5 μM) and ATP (2 mM) at 30°C for 1 h. Phosphorylation of IκBα was detected by immunoblot with an anti-p-IκBα antibody (right). (D) Tax binding to the IKK complex depends on NEMO. The cell-free assay was performed as described in (C), and the reaction mixtures were then subjected to a Ni-NTA pull-down assay to analyse interaction of Tax with the IKK complex subunits by immunoblot with anti-IKKα, anti-IKKβ and anti-NEMO antibodies.

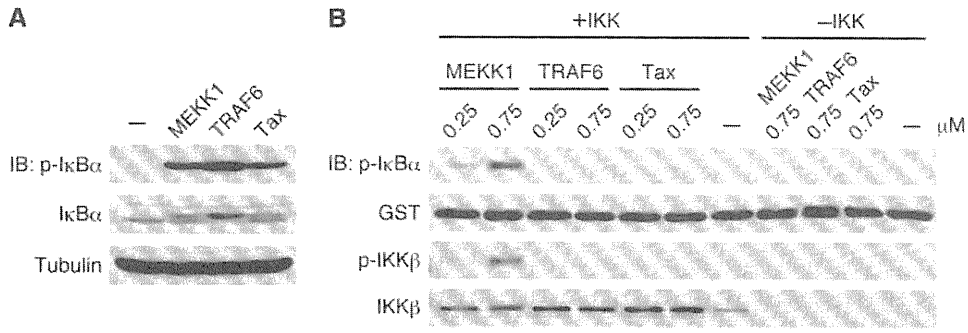

Fig. 3 Tax requires intermediary factors for IKK activation. (A) Recombinant MEKK1, TRAF6 and Tax activated the IKK complex in the Jurkat cytosolic extract. The Jurkat cytosolic extract (10 mg/ml) was incubated with either recombinant MEKK1 (0.75 μM), TRAF6 (0.75 μM) or Tax (0.75 μM) and ATP (2 mM) at 30°C for 1 h. Phosphorylated IκBα was detected by immunoblot with an anti-p-IκBα antibody. (B) Recombinant Tax did not activate the purified IKK complex. Recombinant MEKK1, TRAF6 or Tax was incubated with ATP (2 mM) and GST-IκBα (100 ng) at 30°C for 1 h either without (−IKK) or with (+IKK) the IKK complex purified from unstimulated Jurkat cells. The reaction mixtures were analysed by immunoblot with anti-p-IκBα, anti-GST, anti-p-IKKβ and anti-IKKβ antibodies.

MEKK1 was unable to induce phosphorylation of IκBα without the IKK complex (Fig. 3B, −IKK), indicating that MEKK1 does not directly phosphorylate IκBα. Similar to TRAF6, Tax alone did not activate the purified IKK complex (Fig. 3B), indicating that Tax requires intermediary factors for IKK activation, which are in the Jurkat cell cytosol.

Polyubiquitination is involved in Tax-induced IKK activation but not in the interaction between Tax and NEMO

We next sought to determine that cytosolic intermediary factor(s) required for Tax-induced IKK activation. It has been well established that various polyubiquitin chains are crucial in IL-1- and TNF-α-induced IKK

activation (*7*). IL-1 induces the polyubiquitinated forms of TRAF6 and TAK1, and TNF-α induces those of RIP1 (*8*, *9*, *11*, *12*). Moreover, it has been reported that unanchored polyubiquitin chains are generated in response to these stimulating events (*27*). These polyubiquitin chains act as a platform for the formation of an active TAK1-containing signalling complex, which activates IKK. In addition to TAK1 activation, the activation of IKK requires stimulation-induced Lys63-linked or linear polyubiquitin chain conjugation to NEMO (*28–32*), which may induce either oligomer formation or a conformational change in NEMO to activate the IKK complex. The former conjugation is catalysed by TRAF6 with Ubc13 and the latter by the linear ubiquitin chain assembly complex (LUBAC), which is composed of HOIL-1, HOIP and Sharpin (*33–35*). We have previously shown that Ubc13 is dispensable to Tax-induced IKK activation, and expression of CYLD does not affect Tax-induced NF-κB activation (*15*). However, we cannot exclude the possibility that Lys63-linked polyubiquitination is involved in Tax-induced IKK activation because E2 ubiquitin-conjugating enzymes other than Ubc13 could be involved and that the Lys63-linked polyubiquitin chains could be somehow blocked from CYLD-mediated deubiquitination. Because our cell-free assay system is not affected by the Tax-induced secretion of various cytokines that trigger generation of polyubiquitin chains, we next investigated whether polyubiquitination was required in Tax-mediated IKK activation using the cell-free system. To inhibit polyubiquitin chain formation, we used two ubiquitin mutants. We used a lysine-free ubiquitin mutant, in which all the lysine residues were mutated to arginine (K0-Ub). We also used a methylated ubiquitin, in which the amino groups, including the ε-amino group, on all the lysine residues and the N-terminal Met α-amino group were blocked by methylation (Me-Ub). The addition of these ubiquitin mutants suppressed TRAF6-induced IKK activation, whereas MEKK1-induced IKK activation was not affected (Fig. 4A). This result is consistent with the notion that polyubiquitination is involved in TRAF6-induced IKK activation but not in MEKK1-induced IKK activation (*9*). More importantly, both ubiquitin mutants suppressed Tax-induced IKK activation (Fig. 4A). This result indicates that polyubiquitination is involved in Tax-induced IKK complex activation.

As Tax binding to NEMO is essential for Tax-induced IKK activation (*22*, *23*), we next examined whether the ubiquitin mutants inhibited the interaction between Tax and the IKK complex. The Jurkat cytosolic extract was incubated with recombinant Tax with and without either wild-type ubiquitin or the mutants. An aliquot of the reaction mixture was immunoblotted directly to examine IKK activation, and the remaining mixture was used for Ni-NTA pull-down assays to analyse the interaction between Tax and the IKK complex. Although K0-Ub and Me-Ub inhibited Tax-induced IKK activation as expected (Fig. 4B, left), the addition of these mutants had no effect on the association between Tax and the IKK complex (Fig. 4B, right). These results suggest that the interaction between Tax and the IKK complex is insufficient to induce IKK activation, and there may be additional steps, in which polyubiquitination is involved, for Tax-induced activation of the IKK complex.

As the addition of K0-Ub does not inhibit the generation of linear polyubiquitin chains (*36*), K0-Ub-mediated inhibition of Tax-induced IKK activation suggests that linear polyubiquitination is

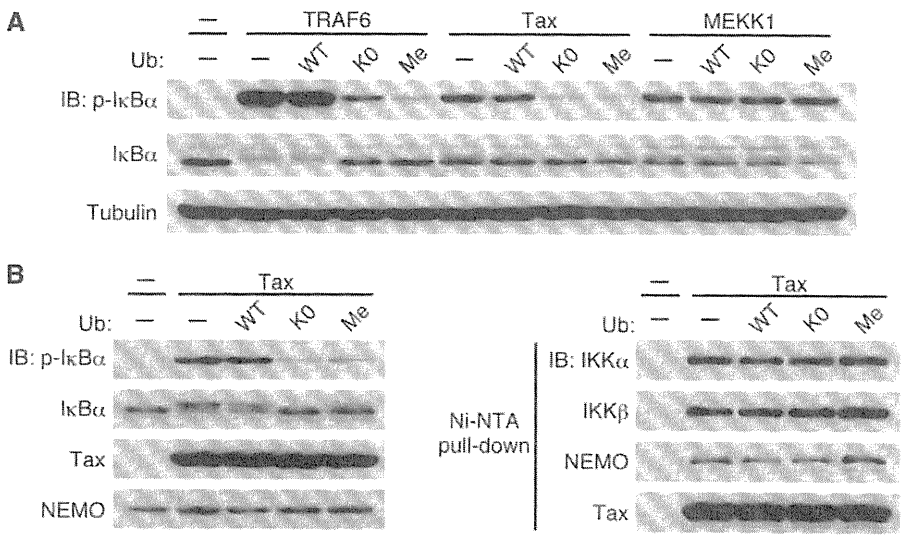

Fig. 4 Polyubiquitination is involved in Tax-induced IKK activation. (A) The Jurkat cytosolic extract (10 mg/ml) was mixed with wild-type (WT, 100 μM), lysine-free (K0, 100 μM), or methylated (Me, 100 μM) ubiquitin and then incubated with recombinant TRAF6 (0.5 μM), Tax (0.5 μM) or MEKK1 (0.5 μM) and ATP (2 mM) at 30°C for 1 h. Phosphorylation of IκBα was detected by immunoblot with an anti-p-IκBα antibody. (B) The Jurkat cytosolic extract (10 mg/ml) was mixed with either WT ubiquitin or the ubiquitin mutants (100 μM), as well as recombinant Tax (0.5 μM) and ATP (2 mM) at 30°C for 1 h. After incubation, aliquots of the reaction mixtures were immunoblotted directly with an anti-p-IκBα antibody to examine IKK activation, and the remaining mixture was used for a Ni-NTA pull down to analyse the interaction between Tax and the IKK complex by immunoblot with anti-IKKα, anti-IKKβ, anti-NEMO and anti-Tax antibodies.

dispensable or insufficient for IKK activation by Tax. These results led us to test whether Lys63-linked polyubiquitination is involved. We first examined whether Tax induces polyubiquitination in the cell-free system. Immunoprecipitation and subsequent immunoblot with an anti-ubiquitin antibody revealed that Tax induces polyubiquitination of Tax and NEMO in the cell-free system (Fig. 5A). The cell-free assay was then performed with the ubiquitin mutant, either K48R or K63R, in which the Lys-48 or Lys-63 of ubiquitin was mutated to Arg, respectively. K48R did not have an effect, but K63R completely inhibited Tax-induced IKK activation (Fig. 5B), which indicates that Lys-63-linked polyubiquitination is required for Tax-induced IKK activation. In the IL-1R and TLR pathways, TRAF6 acts as an E3 ubiquitin ligase to generate K63-linked polyubiquitin chains upon stimulation (*8*, *9*). Therefore, cytosolic extracts were prepared from wild-type MEF cells and *Traf6*$^{-/-}$ MEF cells and then tested for Tax-induced IKK activation. Similar levels of IκBα phosphorylation were observed in the WT and *Traf6*$^{-/-}$ extracts (Fig. 5C), which indicates that TRAF6 is dispensable for Tax-induced IKK activation.

In this study, using a cell-free assay system, we demonstrated that activation of the IKK complex by HTLV-1 Tax requires cytosolic factor(s) that are involved in Tax-induced polyubiquitination. As polyubiquitination is catalysed by three enzymes, E1, E2 and E3 (*37*), it is important to identify these enzymes to further elucidate the molecular mechanisms of Tax-induced IKK activation. Although our results strongly suggest that K63-linked polyubiquitin chains are involved in the Tax-induced IKK activation, TRAF6 does not act as an E3 and the involvement of Ubc13 as an E2 is still controversial (*15*, *16*). It is well known that polyubiquitin chains with different lysine linkages have distinct biological roles (*38*, *39*). Lys48-linked polyubiquitin chains are a signal for proteasomal degradation. On the other hand, Lys63-linked and linear polyubiquitin chains play an important role in the cytokine signal transduction pathway that leads to NF-κB activation. Further studies are required to determine which types of polyubiquitin chain are involved in Tax-induced IKK complex activation. We also found that polyubiquitination was not required for the interaction between Tax and the IKK complex. This result raises the possibility that polyubiquitination might be required either to recruit IKK kinase (IKKK) or to induce *trans*-autophosphorylation of the IKK complex, which induces IKK activation. It has been reported that ubiquitination of Tax is required for the interaction of Tax with NEMO (*16*). Although the reason for the discrepancy

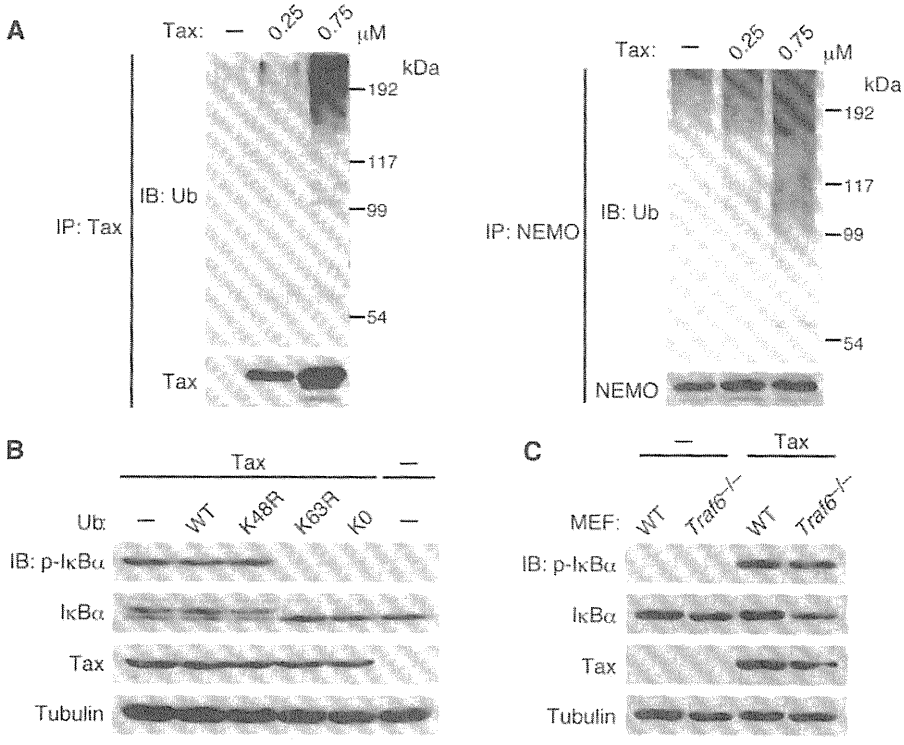

Fig. 5 Potential involvement of Lys-63-linked polyubiquitination in Tax-induced IKK activation. (A) Recombinant Tax induces polyubiquitination of Tax and NEMO in the cell-free system. The Jurkat cytosolic extract (10 mg/ml) was incubated with recombinant Tax with ATP (2 mM) at 30°C for 1 h. After incubation, the reaction mixture was first boiled to remove the non-covalently attached proteins and then immunoprecipitated with either an anti-Tax (left) or anti-NEMO (right) antibody. Ubiquitination of Tax and NEMO was detected by immunoblot with an anti-ubiquitin antibody. (B) The Lys63-linked polyubiquitin chain is involved in Tax-induced IKK activation. The Jurkat cytosolic extract (10 mg/ml) was incubated with recombinant Tax (0.5 μM) and either the WT or ubiquitin mutants (100 μM) with ATP (2 mM) at 30°C for 1 h. IκBα phosphorylation was detected by immunoblot with an anti-p-IκBα antibody. (C) TRAF6 is not involved in Tax-induced IKK activation. Recombinant Tax (0.5 μM) was incubated with the cytosolic extract from either WT or *Traf6*$^{-/-}$ MEFs (10 mg/ml) with (2 mM) at 30°C for 1 h. Phosphorylation of IκBα was detected by immunoblot with an anti-p-IκBα antibody.

is not clear, identification of the polyubiquitinated proteins and IKK-interacting proteins using our cell-free system may provide clues to understanding the molecular mechanisms of Tax-induced IKK activation.

Acknowledgements

We thank S. Okada, A. Nishizawa and K. Shimizu for secretarial assistance.

Funding

The Ministry of Education, Culture, Sports, Science and Technology of Japan (grants-in-aid for Scientific Research on Innovative Areas to J.I.); the Takeda Science Foundation (to J.I.); the Sato Memorial Foundation for Cancer Research (to J.I.).

Conflict of interest

None declared.

References

1. Yoshida, M. (2010) Molecular approach to human leukemia: isolation and characterization of the first human retrovirus HTLV-1 and its impact on tumorigenesis in adult T-cell leukemia. *Proc. Jpn. Acad.* **86**, 117–130
2. Tanaka, A., Takahashi, C., Yamaoka, S., Nosaka, T., Maki, M., and Hatanaka, M. (1990) Oncogenic transformation by the tax gene of human T-cell leukemia virus type I in vitro. *Proc. Natl. Acad. Sci. USA* **87**, 1071–1075
3. Grossman, W.J., Kimata, J.T., Wong, F.H., Zutter, M., Ley, T.J., and Ratner, L. (1995) Development of leukemia in mice transgenic for the tax gene of human T-cell leukemia virus type I. *Proc. Natl. Acad. Sci. USA* **92**, 1057–1061
4. Sun, S.C. and Yamaoka, S. (2005) Activation of NF-κB by HTLV-I and implications for cell transformation. *Oncogene* **24**, 5952–5964
5. Robek, M.D. and Ratner, L. (1999) Immortalization of $CD4^+$ and $CD8^+$ T lymphocytes by human T-cell leukemia virus type 1 Tax mutants expressed in a functional molecular clone. *J. Virol.* **73**, 4856–4865
6. Hayden, M.S. and Ghosh, S. (2008) Shared principles in NF-κB signaling. *Cell* **132**, 344–362
7. Liu, S. and Chen, Z.J. (2011) Expanding role of ubiquitination in NF-κB signaling. *Cell Res.* **21**, 6–21
8. Yamazaki, K., Gohda, J., Kanayama, A., Miyamoto, Y., Sakurai, H., Yamamoto, M., Akira, S., Hayashi, H., Su, B., and Inoue, J. (2009) Two mechanistically and temporally distinct NF-κB activation pathways in IL-1 signaling. *Sci. Signal.* **2**, ra66
9. Deng, L., Wang, C., Spencer, E., Yang, L., Braun, A., You, J., Slaughter, C., Pickart, C., and Chen, Z.J. (2000) Activation of the IκB kinase complex by TRAF6 requires a dimeric ubiquitin-conjugating enzyme complex and a unique polyubiquitin chain. *Cell* **103**, 351–361
10. Kanayama, A., Seth, R.B., Sun, L., Ea, C.K., Hong, M., Shaito, A., Chiu, Y.H., Deng, L., and Chen, Z.J. (2004) TAB2 and TAB3 activate the NF-κB pathway through binding to polyubiquitin chains. *Mol. Cell* **15**, 535–548
11. Mahoney, D.J., Cheung, H.H., Mrad, R.L., Plenchette, S., Simard, C., Enwere, E., Arora, V., Mak, T. W., Lacasse, E.C., Waring, J., and Korneluk, R.G. (2008) Both cIAP1 and cIAP2 regulate TNFα-mediated NF-κB activation. *Proc. Natl. Acad. Sci. USA* **105**, 11778–11783
12. Bertrand, M.J., Milutinovic, S., Dickson, K.M., Ho, W.C., Boudreault, A., Durkin, J., Gillard, J.W., Jaquith, J.B., Morris, S.J., and Barker, P.A. (2008) cIAP1 and cIAP2 facilitate cancer cell survival by functioning as E3 ligases that promote RIP1 ubiquitination. *Mol. Cell* **30**, 689–700
13. Chu, Z.L., Shin, Y.A., Yang, J.M., DiDonato, J.A., and Ballard, D.W. (1999) IKKγ mediates the interaction of cellular IκB kinases with the tax transforming protein of human T cell leukemia virus type 1. *J. Biol. Chem.* **274**, 15297–15300
14. Harhaj, E.W. and Sun, S.C. (1999) IKKγ serves as a docking subunit of the IκB kinase (IKK) and mediates interaction of IKK with the human T-cell leukemia virus Tax protein. *J. Biol. Chem.* **274**, 22911–22914
15. Gohda, J., Irisawa, M., Tanaka, Y., Sato, S., Ohtani, K., Fujisawa, J., and Inoue, J. (2007) HTLV-1 Tax-induced NFκB activation is independent of Lys-63-linked-type polyubiquitination. *Biochem. Biophys. Res. Commun.* **357**, 225–230
16. Shembade, N., Harhaj, N.S., Yamamoto, M., Akira, S., and Harhaj, E.W. (2007) The human T-cell leukemia virus type 1 Tax oncoprotein requires the ubiquitin-conjugating enzyme Ubc13 for NF-κB activation. *J. Virol.* **81**, 13735–13742
17. Kobayashi, N., Kadono, Y., Naito, A., Matsumoto, K., Yamamoto, T., Tanaka, S., and Inoue, J. (2001) Segregation of TRAF6-mediated signaling pathways clarifies its role in osteoclastogenesis. *EMBO J.* **20**, 1271–1280
18. Mori, N. and Prager, D. (1996) Transactivation of the interleukin-1α promoter by human T-cell leukemia virus type I and type II Tax proteins. *Blood* **87**, 3410–3417
19. Cowan, E.P., Alexander, R.K., Daniel, S., Kashanchi, F., and Brady, J.N. (1997) Induction of tumor necrosis factor α in human neuronal cells by extracellular human T-cell lymphotropic virus type 1 Tax. *J. Virol.* **71**, 6982–6989
20. Pierce, J.W., Schoenleber, R., Jesmok, G., Best, J., Moore, S.A., Collins, T., and Gerritsen, M.E. (1997) Novel inhibitors of cytokine-induced IκBα phosphorylation and endothelial cell adhesion molecule expression show anti-inflammatory effects in vivo. *J. Biol. Chem.* **272**, 21096–21103
21. Burke, J.R., Pattoli, M.A., Gregor, K.R., Brassil, P.J., MacMaster, J.F., McIntyre, K.W., Yang, X., Iotzova, V.S., Clarke, W., Strnad, J., Qiu, Y., and Zusi, F.C. (2003) BMS-345541 is a highly selective inhibitor of IκB kinase that binds at an allosteric site of the enzyme and blocks NF-κB-dependent transcription in mice. *J. Biol. Chem.* **278**, 1450–1456
22. Yamaoka, S., Courtois, G., Bessia, C., Whiteside, S.T., Weil, R., Agou, F., Kirk, H.E., Kay, R.J., and Israel, A. (1998) Complementation cloning of NEMO, a component of the IκB kinase complex essential for NF-κB activation. *Cell* **93**, 1231–1240
23. Harhaj, E.W., Good, L., Xiao, G., Uhlik, M., Cvijic, M.E., Rivera-Walsh, I., and Sun, S.C. (2000) Somatic mutagenesis studies of NF-κB signaling in human T cells: evidence for an essential role of IKKγ in NF-κB activation by T-cell costimulatory signals and HTLV-I Tax protein. *Oncogene* **19**, 1448–1456
24. Mukherjee, S., Negi, V.S., Keitany, G., Tanaka, Y., and Orth, K. (2008) In vitro activation of the IκB kinase

complex by human T-cell leukemia virus type-1 Tax. *J. Biol. Chem.* **283**, 15127–15133
25. Lee, F.S., Peters, R.T., Dang, L.C., and Maniatis, T. (1998) MEKK1 activates both IκB kinase α and IκB kinase β. *Proc. Natl. Acad. Sci. USA* **95**, 9319–9324
26. Wang, C., Deng, L., Hong, M., Akkaraju, G.R., Inoue, J., and Chen, Z.J. (2001) TAK1 is a ubiquitin-dependent kinase of MKK and IKK. *Nature* **412**, 346–351
27. Xia, Z.P., Sun, L., Chen, X., Pineda, G., Jiang, X., Adhikari, A., Zeng, W., and Chen, Z.J. (2009) Direct activation of protein kinases by unanchored polyubiquitin chains. *Nature* **461**, 114–119
28. Gautheron, J. and Courtois, G. (2010) "Without Ub I am nothing": NEMO as a multifunctional player in ubiquitin-mediated control of NF-κB activation. *Cell. Mol. Life Sci.* **67**, 3101–3113
29. Ni, C.Y., Wu, Z.H., Florence, W.C., Parekh, V.V., Arrate, M.P., Pierce, S., Schweitzer, B., Van Kaer, L., Joyce, S., Miyamoto, S., Ballard, D.W., and Oltz, E.M. (2008) Cutting edge: K63-linked polyubiquitination of NEMO modulates TLR signaling and inflammation in vivo. *J. Immunol.* **180**, 7107–7111
30. Sebban-Benin, H., Pescatore, A., Fusco, F., Pascuale, V., Gautheron, J., Yamaoka, S., Moncla, A., Ursini, M.V., and Courtois, G. (2007) Identification of TRAF6-dependent NEMO polyubiquitination sites through analysis of a new NEMO mutation causing incontinentia pigmenti. *Hum. Mol. Genet.* **16**, 2805–2815
31. Abbott, D.W., Wilkins, A., Asara, J.M., and Cantley, L.C. (2004) The Crohn's disease protein, NOD2, requires RIP2 in order to induce ubiquitinylation of a novel site on NEMO. *Curr. Biol.* **14**, 2217–2227
32. Tokunaga, F., Sakata, S., Saeki, Y., Satomi, Y., Kirisako, T., Kamei, K., Nakagawa, T., Kato, M., Murata, S., Yamaoka, S., Yamamoto, M., Akira, S., Takao, T., Tanaka, K., and Iwai, K. (2009) Involvement of linear polyubiquitylation of NEMO in NF-κB activation. *Nat. Cell Biol.* **11**, 123–132
33. Gerlach, B., Cordier, S.M., Schmukle, A.C., Emmerich, C.H., Rieser, E., Haas, T.L., Webb, A.I., Rickard, J.A., Anderton, H., Wong, W.W., Nachbur, U., Gangoda, L., Warnken, U., Purcell, A.W., Silke, J., and Walczak, H. (2011) Linear ubiquitination prevents inflammation and regulates immune signalling. *Nature* **471**, 591–596
34. Ikeda, F., Deribe, Y.L., Skanland, S.S., Stieglitz, B., Grabbe, C., Franz-Wachtel, M., van Wijk, S.J., Goswami, P., Nagy, V., Terzic, J., Tokunaga, F., Androulidaki, A., Nakagawa, T., Pasparakis, M., Iwai, K., Sundberg, J.P., Schaefer, L., Rittinger, K., Macek, B., and Dikic, I. (2011) SHARPIN forms a linear ubiquitin ligase complex regulating NF-κB activity and apoptosis. *Nature* **471**, 637–641
35. Tokunaga, F., Nakagawa, T., Nakahara, M., Saeki, Y., Taniguchi, M., Sakata, S., Tanaka, K., Nakano, H., and Iwai, K. (2011) SHARPIN is a component of the NF-κB-activating linear ubiquitin chain assembly complex. *Nature* **471**, 633–636
36. Kirisako, T., Kamei, K., Murata, S., Kato, M., Fukumoto, H., Kanie, M., Sano, S., Tokunaga, F., Tanaka, K., and Iwai, K. (2006) A ubiquitin ligase complex assembles linear polyubiquitin chains. *EMBO J.* **25**, 4877–4887
37. Pickart, C.M. (2001) Mechanisms underlying ubiquitination. *Annu. Rev. Biochem.* **70**, 503–533
38. Pickart, C.M. and Fushman, D. (2004) Polyubiquitin chains: polymeric protein signals. *Curr. Opin. Chem. Biol.* **8**, 610–616
39. Chen, Z.J. and Sun, L.J. (2009) Nonproteolytic functions of ubiquitin in cell signaling. *Mol. Cell* **33**, 275–286

Journal of Medical Virology 83:1641–1649 (2011)

Molecular and Clinical Effects of Betamethasone in Human T-Cell Lymphotropic Virus Type-I-Associated Myelopathy/Tropical Spastic Paraparesis Patients

Carolina Alberti,[1] Luis Cartier,[2] María A. Valenzuela,[1] Javier Puente,[1] Yuetsu Tanaka,[3] and Eugenio Ramirez[4,5]*

[1]*Faculty of Chemical and Pharmaceutical Sciences, Department of Biochemistry and Molecular Biology, University of Chile, Santiago, Chile*
[2]*Faculty of Medicine, Department of Neurological Sciences, University of Chile, Santiago, Chile*
[3]*Department of Immunology, Graduate School and Faculty of Medicine, University of the Ryukyus, Ryukyus, Japan*
[4]*Faculty of Medicine, Program of Virology, ICBM, University of Chile, Santiago, Chile*
[5]*Department of Virology, Public Health Institute of Chile, Santiago, Chile*

There is no effective therapy for human T-cell lymphotropic virus type I (HTLV-I)-associated myelopathy/tropical spastic paraparesis (HAM/TSP). Glucocorticoids are effective to reduce the motor disability in these patients, but its role as anti-spastic drugs is unknown. Here it is reported the use of corticosteroids in HAM/TSP. The goal was to find reliable molecular markers linked to treatment effectiveness. The clinical efficacy of corticosteroids was studied in 22 HAM/TSP. The treatment was a single dose of 7.0 mg of systemic betamethasone. Pre-treatment samples were obtained immediately before steroid administration and post-treatment samples were collected after 5 days. Neurological disability was evaluated by the Osame's Motor Disability Scales. Relative levels of Tax, Foxp3, IL-10, TGF-β, CTLA-4, and GITR mRNA were measured and the percentage of $CD4^+Foxp3^+$ and $CD4^+Tax^+$ populations was quantified in PBMCs by real-time PCR and flow cytometry, respectively. The same parameters were studied in eight untreated carriers. Betamethasone treatment showed neurological improvement in 21 HAM/TSP patients, with one patient without response to treatment. This therapy was associated with a decrease in Tax mRNA load and $CD4^+Tax^+$ T cells in HAM/TSP. Simultaneously, an increase in Foxp3 mRNA and $CD4^+Foxp3^+$ T cell was detected in these patients. The other markers studied had no significant changes after treatment. Clinical improvement in betamethasone-treated HAM/TSP was associated with an inverse relationship between a decrease in Tax and an increase in Foxp3 at the mRNA and protein levels. These results suggest that both Tax and Foxp3 may represent potential biomarkers for drug treatment assessments in HAM/TSP.
J. Med. Virol. 83:1641–1649, 2011.

KEY WORDS: HTLV-I; betamethasone therapy; HAM/TSP

INTRODUCTION

Human T-cell lymphotropic virus type I (HTLV-I) is the etiologic agent of HTLV-I-associated myelopathy/tropical spastic paraparesis (HAM/TSP) [Osame et al., 1986]. This progressive spastic paraparesis without remittances is interpreted as an inflammatory disease [Nakagawa et al., 1995; Uchiyama, 1997], and also as a neurodegenerative disease [Cartier et al., 1997, 2007; Liberski et al., 1999]. Nevertheless, the progression of the disease is still unknown [Oh et al., 2006]. Worldwide the majority of infected individuals remain asymptomatic carriers while approximately 0.25–3.0% of those infected develop HAM/TSP [Kaplan et al.,

Grant sponsor: Fondecyt; Grant number: 1080396; Grant sponsor: Comisión Nacional de Investigación Científica y Tecnológica (Conicyt) from Chile (Support Scholarship for Doctoral Thesis); Grant number: 24090150.

Carolina Alberti and Luis Cartier equally contributed to this work.

*Correspondence to: Eugenio Ramirez, Department of Virology, Instituto de Salud Pública de Chile, Avenida Marathon 1000, Ñuñoa, Santiago, Chile. E-mail: eramirez@ispch.cl

Accepted 9 May 2011
DOI 10.1002/jmv.22131
Published online in Wiley Online Library (wileyonlinelibrary.com).

1990]. There are no effective ways to prevent the development of HAM/TSP. Glucocorticoids are effective to reduce the motor disability in these patients, probably because of their anti-inflammatory properties [Gotuzzo et al., 2004; Verdonck et al., 2007].

The anti-inflammatory and immunosuppressive effects of the corticoids are widely known, but the anti-spastic action of these drugs is less mentioned [Cartier et al., 1977; Cartier and Verdugo, 1988]. Based on the last effect, corticoids have been used to obtain an effective decrease of spasticity in HAM/TSP patients. The repeated use of corticosteroids allowed the selection of 7.0 mg of rapid and slow action betamethasone in a single-dose monthly as a suitable treatment. This small dose of the drug produces defined improvements, increasing the step-length, speed, gait, and balance in HAM/TSP patients; effects on the control of spastic bladder are seen as well. Additionally, patients in long-term treatment show a slower functional deterioration compared with untreated patients [Cartier, 1998]. As a result of these findings, factors that could be involved in this functional improvement were studied.

In HAM/TSP, natural regulatory T cells (nTreg) characterized by the markers $CD4^+CD25^{hi}Foxp3^+$ are the main reservoir of the virus in vivo [Yamano et al., 2004, 2005]. These cells have the function to suppress, through cell–cell contact, the response of effector T cells and antigen-presenting cells in chronic diseases, including those caused by retroviruses [Grant et al., 2006; Roncarolo and Gregori, 2008]. Tax is a viral and cellular transcriptional regulator associated with the progression of HAM/TSP in most cases [Uchiyama, 1997; Nagai and Jacobson, 2001]. In vitro studies have demonstrated a decrease in Foxp3 levels in the presence of Tax protein [Yamano et al., 2004]. The mechanism of this regulation and its implication in the progression of HAM/TSP are still unknown [Yamano et al., 2005; Toulza et al., 2008].

The aim of this work was to find reliable molecular markers for the effectiveness of betamethasone treatment. In order to characterize the immunological and neurological effects of betamethasone in HAM/TSP patients, this study was directed to evaluate the variation of cytokine levels and receptors involved in down-regulate the immune-response as well as the neurological improvement reflected in gait commitment. In this study, a clinical improvement of HAM/TSP patients treated with betamethasone is reported. This improvement is associated with a characteristic molecular pattern of immunological and viral markers. A clear inverse relationship between a decrease in Tax viral protein and an increase in nTreg marker Foxp3 in response to treatment was found. Other immunological markers such as IL-10, TGF-β, CTLA-4, and GITR were also studied to estimate the involvement in immuno-modulator processes, but no correlation was found either between markers or between markers with gait improvement.

MATERIALS AND METHODS

Patients and Healthy Control Subjects

All the experiments were performed in compliance with relevant laws and the University of Chile Ethics Committee guidelines and in accordance with the ethical standards of the Declaration of Helsinki. Informed consent was obtained from all individuals. HAM/TSP patients fulfilled criteria of gait commitment according to The World Health Organization. Patients were evaluated clinically before and after therapy. Motor disability was evaluated by neurologists in each patient visit. Motor dysfunction was evaluated on the basis of the Osame's Motor Disability Score, in which motor dysfunction is graded on the scale from 0 (normal gait and running) to 13 (completely bedridden). EDTA-treated blood was obtained from 22 HAM/TSP patients, 8 asymptomatic carriers (Carriers), and 8 healthy non-infected subjects. All patients were treated with systemic betamethasone in a single dose of 3.0 mg of rapid action betamethasone plus 4.0 mg of slow action betamethasone. Pre-treatment samples were obtained immediately before steroid administration and post-treatment samples were collected after 5 days. Table I shows clinical data of HAM/TSP patients before and after treatment. Carriers were used as a reliable infected control group without neurological manifestations, and healthy non-infected donors were used as non-infected controls. Both control groups were not treated with betamethasone. The Carriers group was characterized by absence of motor disability, a male:female ratio of 1:1 and a mean age of 37.3 ± 10.2. The healthy non-infected group was similar but with a mean age of 32.7 ± 13.6.

PBMCs Isolation

Peripheral blood mononuclear cells (PBMCs) were obtained from 10 ml of EDTA-treated blood by Ficoll–Hypaque density gradient centrifugation; they were washed three times with phosphate-buffered saline (PBS). The number of PBMCs collected varied between 7×10^6 and 10×10^6.

Nucleic Acid Isolation and cDNA Synthesis

RNA was isolated with RNeasy kit (Qiagen, Valencia, CA) from PBMCs according to the manufacturer's protocol. Reverse transcription was performed with Taq-Man reverse transcription in a one-step PCR.

Relative Real-Time PCR

cDNA was synthesized for relative quantitation of Tax, CTLA-4, GITR, IL-10, TGF-β, and Foxp3 transcripts, after and before betamethasone treatment of HAM/TSP patients. Samples from Carriers and non-infected healthy donors were also analyzed. Hypoxanthine ribosyltransferase (HPRT) was used as housekeeping gene. We designed Tax, Foxp3, HPRT,

TABLE I. Clinical Data of HAM/TSP Patients Treated With Betamethasone

Patients	Age	Sex	Disease evolution (years)	OMDS before treatment	OMDS after treatment
1	40	F	3	4	3
2	46	F	3	5	4
3	68	F	14	4	3
4	74	F	9	5	4
5	63	F	12	5	4
6	69	F	12	5	4
7	61	M	17	5	4
8	56	M	7	6	5
9	53	M	5	4	3
10	71	F	17	7	6
11	74	F	20	5	4
12	79	M	25	4	2
13	54	M	12	9	8
14	61	F	16	7	7
15	36	F	11	6	4
16	50	F	10	5	4
17	57	F	10	3	2
18	50	M	18	4	3
19	72	F	12	5	4
20	49	F	24	7	6
21	63	F	14	4	3
22	65	F	15	5	4

Each column shows different parameters related with age, sex, and years of disease evolution. Motor disability stage measured as gait commitment was evaluated before treatment and 5 days after betamethasone administration.
OMDS, Osame's Motor Disability Scales.

and GITR primers using AmplifiX 1.4 software based on sequences reported in GeneBank; Tax: forward primer (5′-ATC CCG TGG AGA CTC CTC AA-3′), reverse primer (5′-CCA AAC ACG TAG ACT GGG TAT CC-3′); GITR: forward primer (5′-CGA GGA GTG CTG TTC CGA GT-3′), reverse primer (5′-TGG AAT TCA GGC TGG ACA CAC-3′); Foxp3: forward primer (5′-AAT GGC ACT GAC CAA GGC TTC ATC T-3′), reverse primer (5′-GTG CCT CCG GAC AGC AAA CA-3′); and HPRT: forward primer (5′-TGC TGA GGA TTT GGA AAG GGT GTT-3′), reverse primer (5′-AGC ACA CAG AGG GCT ACA ATG TGA-3′). Primers for CTLA-4, IL-10, and TGF-β were described previously [Boeuf et al., 2005; Schaub et al., 2006]. PCR products were spanning exon–intron borders in order to avoid amplification of contaminant genomic DNA. cDNA was amplified using Brilliant® II SYBR® Green master mix (Stratagene, Agilent Technologies, Wilmington, DE). When possible, amplifications were carried out in duplicates. Analysis of melting curves showed a single pick for each marker amplified, coincident with the size of PCR products analyzed in agarose gels. Relative quantitation was made with the comparative threshold cycle ($\Delta\Delta C_T$) formula with HPRT as endogeneous housekeeping gene. Carriers were used as control group for calculation of $\Delta\Delta C_T$, having previously compared them with healthy non-infected individuals. It was not possible to compare Tax mRNA levels in both groups because of the lack of Tax gene in healthy non-infected individuals. Data were normalized to the average value of Carriers.

Flow Cytometry

PBMCs for flow cytometry were cultured 14 h in RPMI 1640 (Gibco, Paisley, UK) supplemented with 10% fetal bovine serum (Gibco) and 20 nM Concanamycin A (Sigma–Aldrich, St Louis, MO) in order to inhibit the action of $CD8^+$ cytotoxic T lymphocytes. Cells were harvested and stained with fluorophore-conjugated antibodies against the following antigens: CD4-FITC (BD Biosciences, San Jose, CA), Foxp3-PE (BD Biosciences) and Tax-APC, kindly provided by Dr. Yuetsu Tanaka. For nuclear Foxp3 and Tax staining, cells were permeabilized with fixation and permeabilization reagents (eBiosciences, San Diego, CA). Matched isotype controls were used at the same concentration as the respective antibodies. A three-color flow cytometry in a FACS-CANTO instrument (Beckton Dickinson) was performed; WinMDI 2.9 software was used for data analysis. To calculate mean fluorescence intensity (MFI) the MFI software (University of Massachusetts) was used. Mean fluorescence of each marker over $CD4^+$ subpopulation was used to determine the level of Foxp3 and Tax protein. Values of MFI plotted were divided by 100 to keep the same scale range of the mRNA data.

Statistics

Statistical analysis was made with Graph Pad Prisma 5.0. Data were verified for Gaussian distribution. For evaluating betamethasone effects in HAM/TSP patients, data before and after treatment were compared using Wilcoxon-singed rank test. Kruskal–Wallis test was used for calculation of differences between independent groups. Data are shown as mean ± SD. The Pearson's correlation was used to evaluate relationship between mRNA and protein levels and between cell populations percentage. Differences in P-values of 0.05 or less were considered significant.

RESULTS

Effects of Betamethasone in Relative Expression of Foxp3 and Tax mRNA in PBMCs of HAM/TSP Patients

A significant increase in the relative amounts of Foxp3 mRNA in HAM/TSP patients treated with systemic betamethasone was observed, compared with pre-treatment samples from the same individuals. There was also a statistical difference between amounts of Foxp3 mRNA from pre-treatment patients and Carriers, but not between healthy non-infected individuals and Carriers, or post-treatment samples (Fig. 1A). Samples from 21 HAM/TSP patients treated with betamethasone showed significant decreases in Tax mRNA compared with those from pre-treatment controls (Fig. 1B). Pre-treatment samples of HAM/

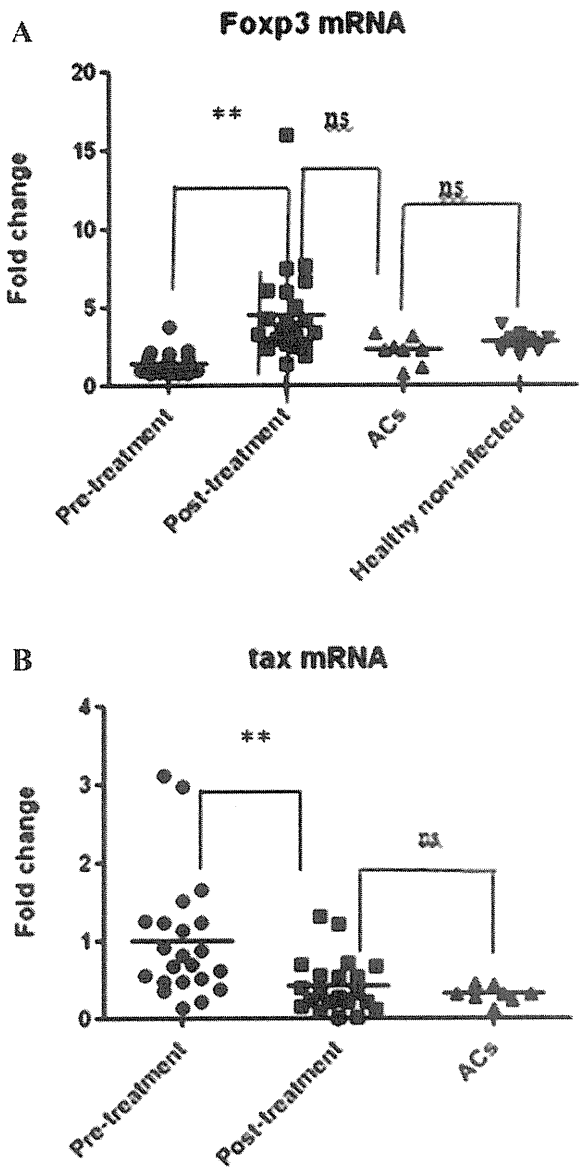

Fig. 1. Fold change of Foxp3 and tax mRNA in HAM/TSP patients treated with betamethasone. **A**: Patients treated with betamethasone showed significant differences in Foxp3 mRNA amounts (4.315 ± 0.73) compared to their pre-treatment condition (1.368 ± 0.16; $^{**}P < 0.0032$). Carriers did not reveal significant differences compared to healthy non-infected controls, as well as with post-treatment samples. **B**: Betamethasone produced a decrease in relative amounts of tax mRNA in HAM/TSP patients (0.469 ± 0.09), in relation to pre-treatment samples (1.039 ± 0.18; $^{**}P < 0.0045$). Relative quantitation of mRNA in Carriers (0.308 ± 0.038) did not show significant differences with post-treatment samples.

TSP showed significant increases compared with those from Carriers. Furthermore, post-treatment HAM/TSP did not show differences from the carriers group. Thus, betamethasone decreased Tax mRNA close to the amounts seen in Carriers. Only patient 14 did not show changes in Tax mRNA levels before and after treatment. Tax mRNA levels were low and similar with those from Carriers.

No significant differences were found in the amounts of mRNA of the immunological markers CTLA-4, GITR, IL-10, and TGF-β in PBMCs from HAM/TSP patients before and after betamethasone treatment, compared with Carriers. There were no statistical differences between these two groups in all analyzed markers (data not shown).

Effect of Betamethasone Treatment in $CD4^+Foxp3^+$ and $CD4^+Tax^+$ Cell Population in HAM/TSP Patients

Betamethasone treatment led to a significant increase in the $CD4^+Foxp3^+$ cell population in 21 HAM/TSP patients compared with pre-treatment controls (Fig. 2A and B). Patient 14 showed a decrease from 2.5 to 1.9% in CD4 $^+Foxp3^+$ cells in pre-treatment and post-treatment samples, respectively. However, the relative amount of Foxp3 mRNA remained similar before and after treatment. No significant differences between the percentages of $CD4^+Foxp3^+$ in carriers, healthy non-infected and HAM/TSP patients post-treatment were observed. Inverse results in the $CD4^+Tax^+$ cell population in response to betamethasone compared to those of $CD4^+Foxp3^+$ cells were found. There was a significant decrease in the percentage of $CD4^+Tax^+$in 21 HAM/TSP-treated patients compared with non-treated controls (Fig. 3A and B). Only patient 14 did not show changes in the percentage of $CD4^+Tax^+$ cells, with similar levels as those of asymptomatic carriers characterized by very low levels of $CD4^+Tax^+$. A comparison of this cell population between Carriers and HAM/TSP-treated patients did not show statistically significant differences. A correlation between $CD4^+Foxp3^+$ and $CD4^+Tax^+$ population before treatment did not show a statistically significant result (data not shown). When data of both cell populations after betamethasone treatment were plotted together, the result was a negative and statistically significant correlation (Pearson's $r = -0.56$; Fig. 4A).

Correlation of mRNA Expression and Protein Levels of Foxp3 and Tax

To support the findings at the mRNA level related with Foxp3 and Tax levels, a correlation between protein and mRNA for each marker was made. Foxp3 and Tax showed both a positive and statistically significant correlation between mRNA expression and protein levels in HAM/TSP patients before and after treatment (Fig. 4B and C). Tax and Foxp3 mRNA of PBMCs from patients before treatment did not show a statistically significant correlation. Instead, the evaluation of Tax and Foxp3 mRNA after the treatment revealed a significant negative correlation with a Pearson's $r = -0.55$ (data not shown).

DISCUSSION

Effective treatment strategies for HAM/TSP are still a challenge and clinical studies available are not enough to support their therapeutic effects. Most

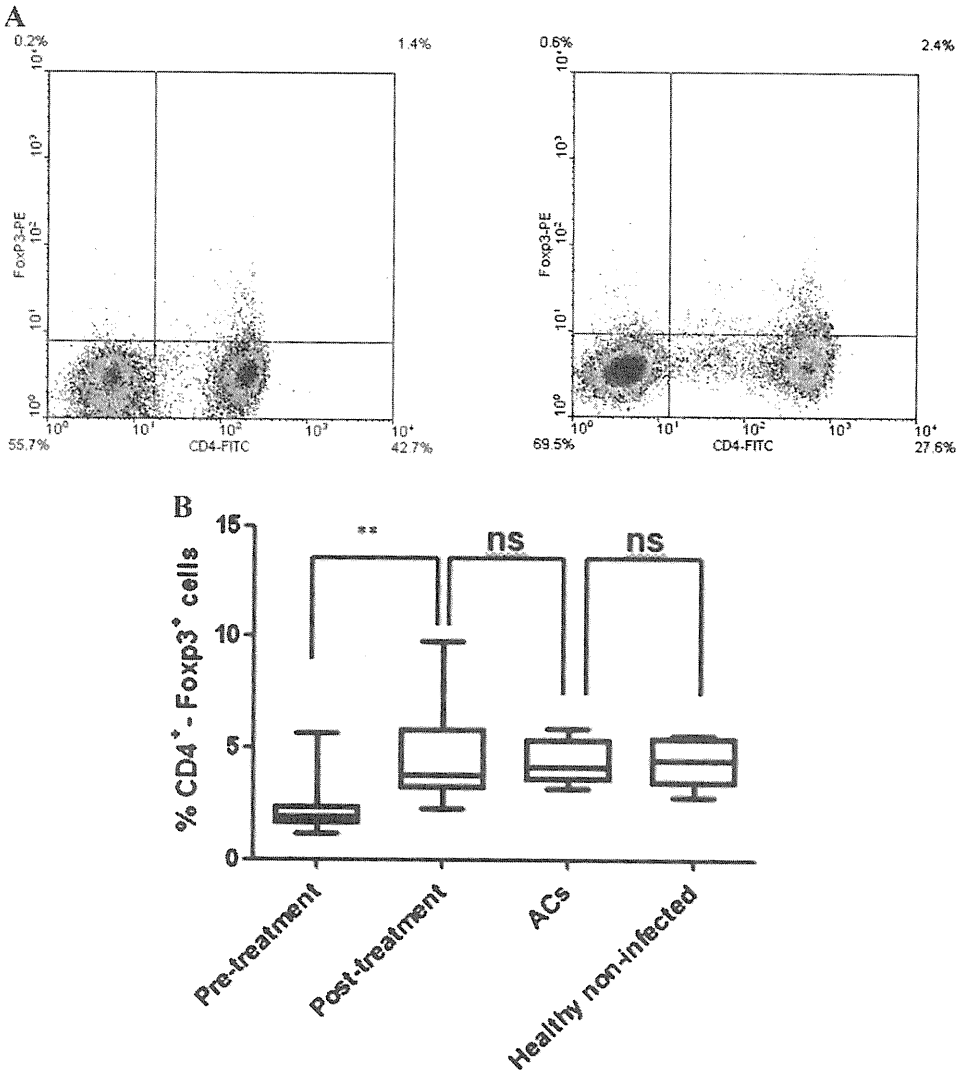

Fig. 2. Flow cytometry analysis of $CD4^+Foxp3^+$ population in HAM/TSP patients treated with betamethasone. Percentage of Treg population was obtained from PBMCs collected from HAM/TSP patients before treatment and 5 days after betamethasone administration. Data were also compared with PBMCs from Carriers and healthy non-infected controls. **A**: Dot-plot representation of $CD4^+Foxp3^+$ population obtained from a pre-treatment sample (*left*) and post-treatment sample (*right*). **B**: Comparison of results from different groups analyzed. Significant differences were found between pre-treatment (2.33 ± 1.24) and post-treatment (5.01 ± 2.24) conditions ($^{**}P < 0.0036$). Post-treatment patients did not show significant differences compared to Carriers (4.34 ± 1.01) and healthy non-infected controls (4.44 ± 1.03).

therapies are symptomatic, being focused on reducing the inflammatory response in affected tissues. Interferon-α (IFN-α), which has both cytostatic and antiviral activity has been used as a potential therapy for HAM/TSP, but with modest results in reducing HTLV-I proviral load [Izumo et al., 1996; Nakagawa et al., 1996; Feng et al., 2003, 2004]. This decrease would be associated with changes in the number of $CD8^+$ T cells [Saito et al., 2004]. Alternative treatments such as oral prednisolone, intrathecal hydrocortisone [Kira et al., 1991; Araujo et al., 1995; Nakagawa et al., 1996], plasmapheresis, and intravenous gammaglobulin have been used [Matsuo et al., 1988; Kuroda et al., 1991; Gold et al., 2007]. Nevertheless, they have not shown clear beneficial effects. The use of antiretroviral drugs including zidovudine and lamivudine has not reported clinically significant changes in 16 patients in a randomized, double-blind study [Taylor et al., 2006]. Even though other kinds of glucocorticoids have been used in HAM/TSP, the advantages of the treatment presented in this work are based on the following characteristics: (a) betamethasone has no interaction with mineralocorticoid receptors, thus there is a higher concentration interacting with glucocorticoid receptors compared with other drugs [Habib and Safia, 2009]; (b) the equivalent dosage compared with other glucocorticoids is eight times less; (c) patients treated with

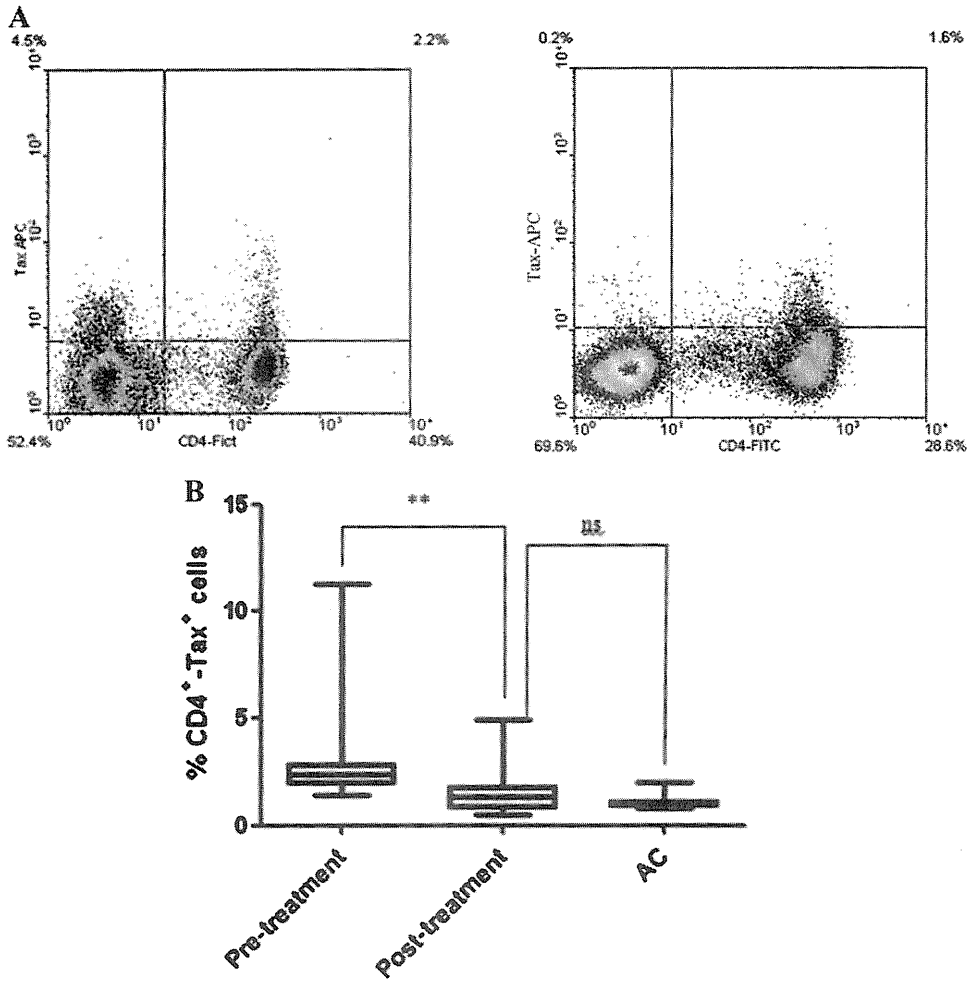

Fig. 3. Quantitation of $CD4^+Tax^+$ population in HAM/TSP patients under betamethasone treatment. PBMCs obtained from HAM/TSP patients before and after treatment as well as from Carriers, were used to quantify $CD4^+Tax^+$ cells and to evaluate the effect of systemic betamethasone in this population. We used Carriers as control group, considering that their $CD4^+Tax^+$ levels are very low and manifestation of motor disability are absent in this individuals. **A**: Dot-plot analysis of a pre-treatment sample (*left*) and post-treatment sample (*right*) highlighting the percentage of $CD4^+Tax^+$ cells. **B**: Results show a statistical difference between pre-treatment (3.03 ± 2.79) and post-treatment (1.43 ± 1.23) conditions ($^{**}P < 0.0038$). No statistical differences were observed when post-treatment and Carriers individuals were compared.

betamethasone do not develop hypertension and features related with this condition; (d) betamethasone has the longest half-life compared with other glucocorticoids; (e) the drug formulation with phosphate and acetate salts increases its bioavailability; (f) a single unique dose is effective for ameliorate disease symptoms; (g) patients do not show secondary effects related with corticoid usage like polyuria, polydipsia, and polyphagia (NIH Clinical Trials). These data were obtained from experimental database (http://www.cancer.gov/Search/ClinicalTrialsLink.aspx?id=39273&idtype=1" active clinical trials) and from clinical observation of patients in this study.

The action of glucocorticoids as immune-modulators in chronic diseases by increasing Foxp3 is well documented [Karagiannidis et al., 2004; Braitch et al., 2009]. It has been suggested that HAM/TSP patients present a reduced Foxp3-dependent suppression capacity [Grant et al., 2008]. This study showed that HAM/TSP patients treated with betamethasone exhibit an increase in Foxp3 mRNA and $CD4^+Foxp3^+$ T cell population at levels comparable with those of non-infected individuals and Carriers. It remains to establish if glucocorticoids-dependent Foxp3 up-regulation leads to a recovery in Treg function compared to Treg obtained from pre-treated HAM/TSP patients. Foxp3 regulatory properties only become active if the immunological environment lacks of danger signals or immune responses are exhausted [Karagiannidis et al., 2004]. Thus, the relatively high levels of pro-inflammatory cytokines or inflammatory-signals present in HAM/TSP might explain the Treg response observed in these patients. A positive correlation was observed between the mRNA expression